6-1-2000

Global system of rivers: Its role in organizing continental land mass and defining land-to-ocean linkages

Charles J. Vorosmarty
University of New Hampshire, Durham, charles.vorosmarty@unh.edu

Balazs M. Fekete
University of New Hampshire, Durham

M. Meybeck
Université de Paris

Richard B. Lammers
University of New Hampshire, Durham, richard.lammers@unh.edu

Recommended Citation

Vorosmarty, C.J., B.M. Fekete, M. Meybeck and R.B. Lammers (2000c) Global system of rivers: Its role in organizing continental land mass and defining land-to-ocean linkages, Global Biogeochemical Cycles, 14(2):599-621.

GLOBAL BIOGEOCHEMICAL CYCLES, VOL. 14, NO. 2, PAGES 599-621, JUNE 2000

Global system of rivers: Its role in organizing continental land mass and defining land-to-ocean linkages

C. J. Vörösmarty[1] and B. M. Fekete[1]

Institute for the Study of Earth, Oceans, and Space, University of New Hampshire, Durham

M. Meybeck

Unité Mixte de Recherche (SISYPHE), Centre National de Recherche Scientifique, Université de Paris VI, Paris

R. B. Lammers

Institute for the Study of Earth, Oceans, and Space, University of New Hampshire, Durham

Abstract. The spatial organization of the Earth's land mass is analyzed using a simulated topological network (STN-30p) representing potential flow pathways across the entire nonglacierized surface of the globe at 30-min (longitude × latitude) spatial resolution. We discuss a semiautomated procedure to develop this topology combining digital elevation models and manual network editing. STN-30p was verified against several independent sources including map products and drainage basin statistics, although we found substantial inconsistency within the extant literature itself. A broad suite of diagnostics is offered that quantitatively describes individual grid cells, river segments, and complete drainage systems spanning orders 1 through 6 based on the Strahler classification scheme. Continental and global-scale summaries of key STN-30p attributes are given. Summaries are also presented which distinguish basins that potentially deliver discharge to an ocean (exorheic) from those that potentially empty into an internal receiving body (endorheic). A total of 59,122 individual grid cells constitutes the global nonglacierized land mass. At 30-min spatial resolution, the cells are organized into 33,251 distinct river segments which define 6152 drainage basins. A global total of 133.1×10^6 km^2 bear STN-30p flow paths with a total length of 3.24×10^6 km. The organization of river networks has an important role in linking land mass to ocean. From a continental perspective, low-order river segments (orders 1-3) drain the largest fraction of land (90%) and thus constitute a primary source area for runoff and constituents. From an oceanic perspective, however, the small number (n=101) of large drainage systems (orders 4-6) predominates; draining 65% of global land area and subsuming a large fraction of the otherwise spatially remote low-order rivers. Along river corridors, only 10% of land mass is within 100 km of a coastline, 25% is within 250 km, and 50% is within 750 km. The global mean distance to river mouth is 1050 km with individual continental values from 460 to 1340 km. The Mediterranean/Black Sea and Arctic Ocean are the most land-dominated of all oceans with land:ocean area ratios of 4.4 and 1.2, respectively; remaining oceans show ratios from 0.55 to 0.13. We discuss limitations of the STN-30p together with its potential role in future global change studies. STN-30p is geographically linked to several hundred river discharge and chemistry monitoring stations to provide a framework for calibrating and validating macroscale hydrology and biogeochemical flux models.

1. Introduction

The land-based water cycle is an integral part of the Earth system, helping to regulate land-atmosphere interactions, the productivity and biogeochemistry of the terrestrial biosphere, and the long-term dynamics of the geologic cycle. The drainage basin is a natural organizing framework through which distinct elements of the terrestrial water cycle can be analyzed. Watershed analysis, carried out over well-circumscribed landscapes, has served as the foundation for our current understanding of process-level hydrology at the local scale. Also, as demonstrated through previous macroscale water budget studies [*Willmott et al.*, 1985; *Vörösmarty et al.*, 1989; *Mintz and Serafini*, 1989; *Roads et al.*, 1994; *Kite et al.*, 1994; *Oki et al.*, 1995], the inherent advantages of such an approach can be realized as well over large spatial domains. By their very nature, drainage basins integrate complex land surface processes and thereby transform spatially distributed

[1]Also at Earth Sciences Department, University of New Hampshire, Durham.

Paper number 1999GB900092.
0886-6236/00/1999GB900092$12.00

hydrologic fluxes into coherent discharge signals focused within well-bounded river corridors. From a modeling perspective this offers the opportunity to exploit one of the best monitored and least error-prone observations associated with the terrestrial water cycle, namely, time series of measured river discharge.

More recently, the advent of high-resolution digital elevation models (DEMs) like the U.S. Geological Survey (USGS) 30 m topographic series [*U.S. Geol. Surv.*, 1990] and affiliated software products (ARC/INFO, Environmental Systems Research Institute, Inc. [ESRI], Redlands, California; Geographic Resources Analysis Support System (GRASS), U.S. Army Corps of Engineers Laboratory, Champaign, Illinois) has facilitated automated derivation of detailed stream networks and analysis of drainage basin characteristics. Despite this availability of data, an articulation of the interactions that link river systems, geomorphology, and the terrestrial water cycle awaits study at continental and global scales. In addition, although several global studies of water balance [*Baumgartner and Reichel*, 1975; *Korzoun et al.*, 1978] and water resources [*L'vovich and White*, 1990; *Shiklomanov*, 1997] are available, none have been placed into a drainage basin or river networking perspective. Further, the use of digital drainage basin information to compute continental to global-scale fluxes of riverborne constituents has only recently begun to be formulated [*White et al.*, 1992; *Esser and Kohlmaier*, 1991; *Ludwig and Probst*, 1998; *Seitzinger and Kroeze*, 1998]. Carefully documented digital data sets representing drainage basins and river networks have been identified as critical needs in the analysis of fluvial constituent transport, for example by the International Geosphere-Biosphere Program (IGBP) [*Vörösmarty et al.*, 1997a] and its newly-created IGBP Water Group.

As a means of facilitating drainage basin analysis at the macroscale, we present in this paper a gridded river networking scheme, global in domain and organized at 30-min spatial resolution. Our data set represents the world's rivers as a collection of Simulated Topological Networks which we refer to as the STN-30p. Details are offered on the construction and verification of this database, its geographic coregistration to discharge and river chemistry monitoring stations, and a set of summary statistics quantifying land-to-ocean linkages. Versions of this network have been applied in water budget and river discharge studies at regional [*Vörösmarty et al.*, 1996a, 1991] and continental scales (R.B. Lammers et al., An assessment of the contemporary gauged river discharge and runoff in the Pan-Arctic region, submitted to *Journal of Geophysical Research*, 2000). In a global context, it has been used to study the impact of large reservoirs on continental runoff and suspended sediment flux [*Vörösmarty et al.*, 1997b, c] and to generate a contemporary climatology of runoff [*Fekete et al.*, 1999]. This paper describes both the current limitations of this 30-min topology as well as its role in future Earth system studies.

Our fundamental aim has been to offer a carefully verified product of practical use to the global change research community, rather than to develop an optimized methodology for automating the derivation of stream networks at the global scale. In this context, when we discuss "simulated" river networks we refer to a digitized representation of river systems operating in the natural world, rather than to any product generated by a simulation model. We present through STN-30p a set of "potential" river networks whose characteristics are established primarily through topography. These networks are distinct from "active" rivers which constitute a subset of the potential networks determined by climate. We emphasize that our analysis is specific to the 30-min spatial scale and that some of the derived statistics could change substantially as a function of grid resolution. The STN-30p data set complements recently developed digital river networks [*Graham et al.*, 1999; *Oki and Sud*, 1998] with global coverage, including an emerging high-resolution 1-km data set (see HYDRO1K: Elevation derivative database available at http://edcwww.cr.usgs.gov/landdaac/gtopo30/hydro/index.html).

2. Division of Continental Land Mass

2.1. Potential Versus Active River Networks

The primary networking scheme described in this paper represents a potential river system topology, under which essentially all land-based grid cells are assigned a directionality with respect to horizontal transport and organized into individual drainage basins. Exceptions to this rule are individual grid cells representing the endpoints of major land-locked drainage systems. In addition, Antarctica, Greenland, portions of the Canadian Arctic Archipelago, and other major glacierized areas have not been considered here. STN-30p provides a pathway for the transport of river water across any remaining portion of the globe should sufficient runoff be made available. Thus STN-30p specifies river networks across dry regions, where no contemporary river discharge nor active channel networks exist today, but whose underlying topography shows no apparent reason for significant water storage on land. River networks in STN-30p also include flow pathways through large inland water bodies such as the Great Lakes.

Runoff and river discharge ultimately control the connection of continental land mass to the world's oceans. Since the availability of runoff is dynamic over both historical and geological timescales [e.g., *Hartmann*, 1994], it would be desirable to generate a fully evolvable topological structure including the time-varying nature of rivers and lakes [*Coe*, 1997, 1998]. Although this is beyond the scope of our work here, major endpoints along the continuum of runoff availability and associated extent of actively discharging river systems can be simulated using current capabilities. STN-30p represents the first such endpoint under which the fundamental character of its potential river networks is controlled by topography. The second endpoint represents contemporary, actively discharging river networks (STN-30ac). We applied a 3 mm yr^{-1} threshold for runoff above which river systems are assumed to maintain perennial channels. This threshold was obtained from [*Meybeck*, 1995] and confirmed through inspection of nearly 1000 discharge time series given by *Vörösmarty et al.* [1996b, 1998a]. STN-30ac is effectively a subset of the STN-30p potential networking scheme, transformed by contemporary climate and the spatial distribution of present-day runoff. We apply the STN-30ac briefly in the context of network verification as described in section 3.

2.2. Classification of Landmass Into Exorheic and Endorheic Zones

The fundamental structure of the STN-30p is defined by potential flow pathways that empty to either an ocean or inland receiving body. The majority of STN-30p flow pathways connect the interior of the continents to one of four oceans (i.e., Arctic, Atlantic, Pacific, or Indian) or the Mediterranean/Black Sea. These

STN-30p river networks and associated drainage basins are classified as exorheic and will be used later in section 4.2 to derive ocean basin summary statistics for presently active as well as dry river systems like those throughout much of the Sahara. An additional set of river systems is classified as endorheic, representing major land-locked receiving waters (e.g., Caspian and Aral Seas, Great Salt Lake, Lake Chad, and Lake Titicaca) and large topographic depressions located in extremely dry regions (e.g., Altiplano in the Andes, Takla Makan in western China). Within each exorheic or endorheic basin, STN-30p depicts potential flow paths plus the location of a single river mouth.

We recognize that long-term changes in the structure of river systems are linked to the availability of water and hence the spatial characteristics of climate. Our purpose here is to identify endorheic basins and their associated receiving bodies under a contemporary or near-contemporary condition, namely climate spanning the recent past as well as the next several decades.

3. Network Construction

3.1. Initial Network Configuration

The University of New Hampshire - Global Hydrological Archive and Analysis System (UNH-GHAAS) provided the Geographic Information System (GIS) framework for this study. The Simulated Topological Network for potential flow pathways is a global data set derived initially from spatial aggregation to 30-min (longitude × latitude) of the Global Gridded Elevation and Bathymetry (ETOPO5) 5-10 min DEM [*Edwards*, 1989]. The aggregated DEM was used in conjunction with an algorithm (ARC/INFO) that determined a maximum topographic gradient for each land-based grid cell as well as a provisional direction of flow. Flow directions into each cell were assigned as single line links from adjacent upstream pixels. Each directed link was given one of eight compass directions (N, NE, E, SE, S, SW, W, or NW) [*Burrough*, 1986]. A single direction of exit was assigned to each cell; inputs could be from any or all of the remaining directions.

The initial directionality yielded numerous inconsistencies with respect to the location of stream lines in nature, reflecting well-known limitations of the ETOPO5 data set [*Jenson*, 1991; *Band and Moore*, 1995; *Hagemann and Dümenil*, 1998; *Oki and Sud*, 1998]. Further, many of the river networks were stranded in artificial pits, even along well-established river courses. In addition, the land-ocean interface along complex coastlines was sometimes difficult to establish using the automated procedures at 30-min spatial resolution.

To overcome these inconsistencies, the GHAAS was employed to manually reconfigure the network structure and to ensure that simulated river courses adhered to those depicted by a set independent map sources. These included several atlases [*Bartholemew et al.*, 1988, 1994], regional maps [e.g., *Dubief*, 1953], 1:1 million scale Operational Navigation Charts [*Defense Mapping Agency Aerospace Center (DMAAC)*, 1980-86] and their electronic representation through the Digital Chart of the World (DCW) [*Environmental Systems Research Institute (ESRI)*, 1993], and 1:3 million scale ARC/World digitized rivers [*Environmental Systems Research Institute (ESRI)*, 1992]. In keeping with the notion of a potential river network topology, we forced the STN-30p through 209 small topographic pits embedded within the DEM along river courses located in dry regions. We reasoned that these would provide little impedance to river flow should sufficient runoff be made available, based on the similarity of their size distribution to that of 629 such depressions found along actively discharging rivers in STN-30ac and independent maps.

3.2. Derivation of Network Attributes

Several quantitative measures of individual STN-30p river systems and their associated drainage basins were computed. The GHAAS was used to generate continental, ocean basin, and global summaries of drainage basin attributes and with ARC/INFO to generate map products. Drainage basins and subbasins are defined as collections of topologically connected grid cells. Stream order is based on *Strahler* [1964, 1957] and assigned to individual interior links where each link is defined as a single linear pathway connecting an adjacent pair of grid cells. An ordered river segment is defined as an individual set of contiguous, linked grid cells having identical order. The linkage of individual grid cells in STN-30p permits ordered searches to be performed on any river system and attributes to be derived for subbasins associated with any point in the topological structure. This facility was used to determine for each drainage basin: (1) the order of mainstem, (2) the basin area, and (3) the length of mainstem. We also computed length to river mouth for all interior grid cells.

All grid cell areas were computed as a function of latitude (3091 km^2 at the equator, 2176 km^2 at 45°). The mainstem river was identified using an upstream search procedure guided by the maximum in calculated drainage area whenever alternative upstream flow pathways were encountered. The downstream endpoint of the highest-order river segment defines the order of a drainage basin as well as the position of its basin mouth. One estimate of basin length simply assigned the length of the mainstem river course. A second method assigned the single longest flow pathway within each STN-30p drainage basin. All length-related computations accounted for both latitude and curvature of the Earth but not for fine-scale sinuosity. Glacierized land mass was removed from the STN-30p based on inspection of the map sources listed above (section 3.1).

3.3. Verification of Networks and Additional Correction Procedures

In addition to the error-checking procedures applied during initial network configuration, a subsequent verification was based on comparison of STN-30p network and catchment attributes to those derived from previously published sources.

3.3.1. Independent data sets coregistered to STN-30p. A digital river discharge database and monitoring station attribute file (United Nations Educational, Scientific, and Cultural Organization/Global River Discharge Data Set [UNESCO/RivDIS] version 1.1) [*Vörösmarty et al.*, 1998a, 1996b] drawn from published compilations [*United Nations Educational, Scientific, and Cultural Organization - International Hydrological Programme (UNESCO-IHP)*, 1965-1984, 1995] was geographically coregistered to the STN-30p. We used 743 RivDIS stations which we judged to be most reliable for upstream basin area. Using a Water Balance/Transport Model (WBM/WTM) driven by spatial variations in climate forcings [see *Vörösmarty et al.*, 1998b, 1996a], we developed the STN-30ac. We estimate that 78% or 72.6 × 10^6 km^2 of the global, nonglacierized land area that actively

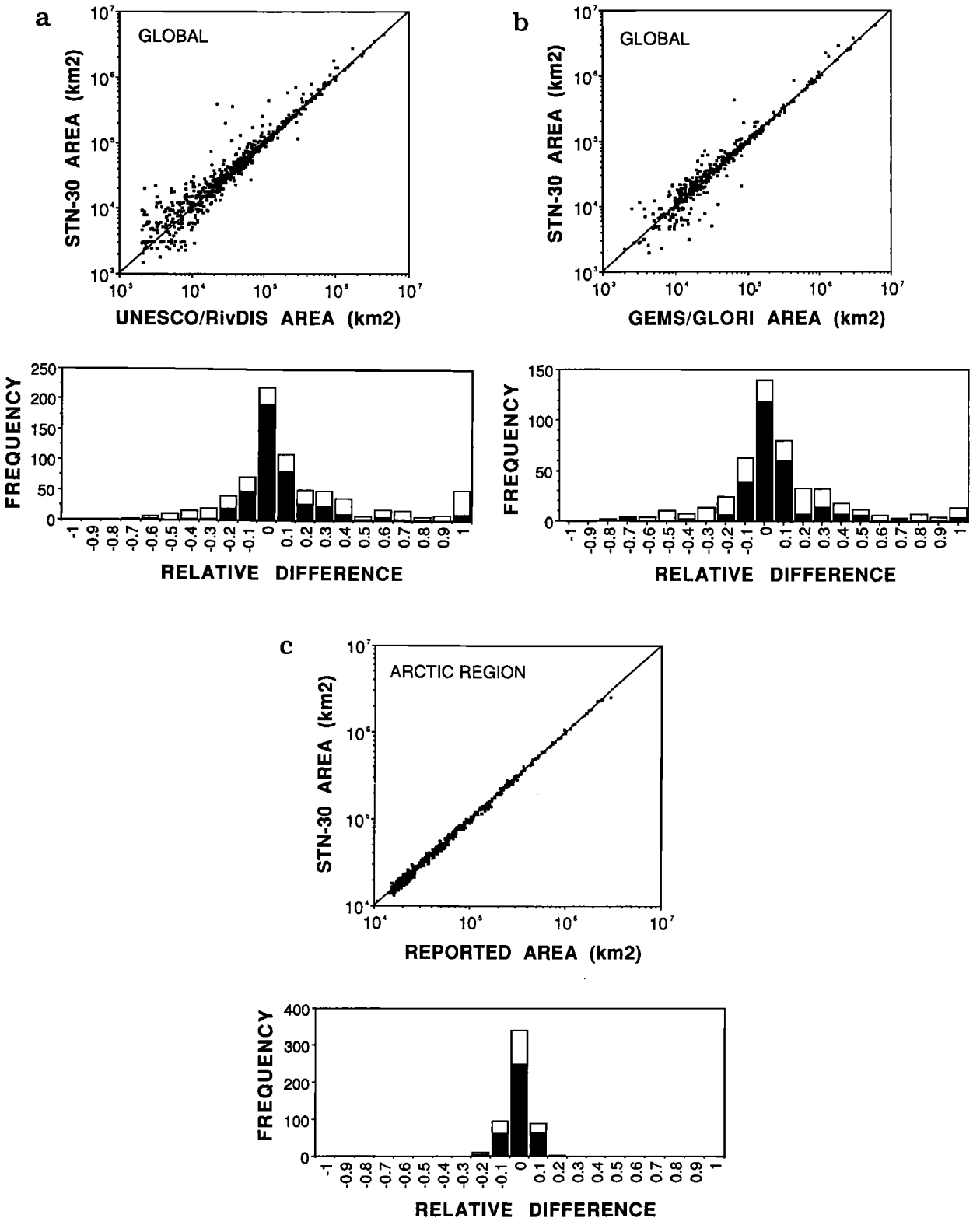

Figure 1. Drainage basin areas derived from STN-30p plotted against reported drainage basin areas from (a) UNESCO-based RivDIS v1.1 stations (n=743) [*Vörösmarty et al.*, 1998a, 1996b], (b) GEMS/GLORI (n=475) [*Meybeck and Ragu*, 1995], and (c) Hydat version 4.93 [*Environment Canada*, 1994], the National Water Resources Data Bank [*State Hydrological Institute*, 1997], and the Water Resources for Alaska data set [U.S. Geol. Surv. 1967-96] (n=538). The 1:1 line is shown in each plot. Frequency distributions of relative difference are partitioned into basins above and below 25,000 km^2 (black and white portions of each histogram bar, respectively). The plot in Figure 1c demonstrates the accuracy of STN-30p when compared to well-documented, standardized estimates of basin area.

Table 1. Basin Area Discrepancies in Extant Literature

River Basin	Country	Continent	Previously Reported Area: Minimum, 10^3 km^2	Previously Reported Area: Maximum, 10^3 km^2	Range,* %	STN-30p Area, 10^3 km^2
		>250 × 10^3 km^2 (from STN-30p)				
Ob	Russia	Europe	2430	2990	23	2570 (1)
St. Lawrence	Canada/USA	North America	1026	1290	26	1043 (1)
Shatt Arab	Iraq	Asia	541	923	71	967 (2)
Orange	South Africa	Africa	604	1020	69	944 (2)
Senegal	Senegal	Africa	268	441	65	847 (2)
Rio Grande	USA/Mexico	North America	467	870	86	805 (2)
Limpopo	Mozambique	Africa	196	440	124	420 (2)
Uruguay	Uruguay	South America	240	310	29	356 (1)
Pechora	Russia	Europe	248	324	31	302
		100 × 10^3 km^2 to 250 × 10^3 km^2				
Huai	China	Asia	164	270	65	244 (3)
Olenek	Russia	Asia	181	219	21	212
Negro	Argentina	South America	97	130	34	198 (2)
Chubut	Argentina	South America	79	140	77	197 (2)
Hong	Vietnam	Asia	120	165	38	171
Rhine	Netherlands	Europe	160	224	40	165 (1)
Essequibo	Guyana	South America	68	164	141	148 (1)
Chao Phrya	Thailand	Asia	111	177	59	142 (1)
Mahanadi	India	Asia	89	142	59	141
Pyasina	Russia	Asia	125	182	46	139 (1)
Adour	France	Europe	16	78 (4)	389	135
Taz	Russia	Asia	100	150	50	129 (1)
Narmada	India	Asia	99	121	22	114
Severn	Canada	North America	101	191	89	104
		<100 × 10^3 km^2				
Tana	Kenya	Africa	42.0	91.0	117	98.9 (2)
Cunene	Angola	Africa	106.5	137.0	29	98.1
Hayes	Canada	North America	103.0	198.0	92	94.0
Daugava	Latvia	Europe	64.5	87.9	36	83.4
Mamberamo	Indonesia	Asia	52.7	77.6	47	77.1
Sacramento	USA	North America	55.0	70.0	27	75.8 (1)
Seine	France	Europe	60.0	78.6	31	73.5 (1)
Gambia	Gambia	Africa	42.0	180.0	329	72.2 (1)
Dnestr	Ukraine	Europe	43.0	72.1	68	72.0
Bug	Ukraine	Europe	46.0	63.7	38	69.2
Alazeya	Russia	Asia	29.0	68.0	134	63.0
Tapti	India	Asia	49.0	65.9	34	66.3
San Joaquin	USA	North America	35.0	80.0	129	60.1
Cheliff	Algeria	Africa	29.3	43.7	49	58.0
Evros	Greece/Turkey	Europe	27.0	55.0	104	55.1
Saint John	Canada	North America	39.9	55.4	39	53.0
Nadym	Russia	Asia	48.0	64.0	33	53.0
Oueme	Benin	Africa	23.6	50.0	112	52.0 (1)
Arnaud	Canada	North America	27.0	49.5	83	51.2 (1)
Ceyhan	Turkey	Asia	15.0	22.0	47	34.2
Delaware	USA	North America	17.6	29.5	68	29.5 (1)
Mahi	India	Asia	25.5	37.6	47	28.5
Ntem	Cameroun	Africa	18.0	31.0	72	27.8
Nass	Canada	North America	20.7	55.0	166	20.6
Thames	Great Britain	Europe	9.9	15.3	55	17.3 (1)
Ems	Germany	Europe	1.3	5.1	292	1.9 (1)

The range in estimates of basin area is given below for several individual river systems as reported in the GEMS/GLORI data set [*Meybeck and Ragu*, 1995, 1997]. These examples represent a subset of all basins for which duplicate entries exist, ranked by STN-30p area. All entries below show disparities in excess of 20%. The numbers in parentheses offer likely reasons for the apparent disparities among reported areas. (1) Problem in defining limit of estuary; (2) nondischarging portions of basin not consistently included in total area; (3) lower river course is unstable or artificial; and (4) incorrect entry in GEMS/GLORI.

*Although this computed range is calculated on the minimum and maximum reported areas in GEMS/GLORI, the *Meybeck and Ragu* [1995, 1997] database does offer a preferred entry for each river. Range percent is computed here as 100 × (Maximum/Minimum - 1.00).

contributes continental runoff (93.1×10^6 km^2) is represented by the in situ RivDIS monitoring data employed in this study.

Another source of station-based statistics was provided by a global data archive organized under the Global Environmental Monitoring System (GEMS) - Water Programme of the World Health Organization (WHO) and United Nations Environment Programme (UNEP). The GEMS/Global River Inputs to the Ocean (GLORI) digital archive [*Meybeck and Ragu*, 1995, 1997] is a compendium of observational data from more than one thousand original literature entries describing drainage basin attributes, runoff and discharge, and waterborne constituents. The data are basin scale and represent conditions at river mouths. We geographically coregistered the 530 GEMS/GLORI stations to the STN-30p to enable direct comparison of contributing areas (n=475) and river lengths (n=299).

For the region of the Arctic, STN-30p basin areas were compared to those from 538 monitoring stations abstracted from Hydat version 4.93 [*Environment Canada*, 1994], the Russian National Water Resources Data Bank [*State Hydrological Institute*, 1997], and the Water Resources for Alaska data set [*U.S. Geol. Surv.*, 1967-1996]. These data represent sites exclusively within the 17×10^6 km^2 watershed that empties into the Arctic Ocean.

3.3.2. Basin area comparisons. Potential drainage basin areas in STN-30p were compared to areas reported at UNESCO/RivDIS gauging stations (Figure 1a). Overall, the median and mean disparities between the two data sets were ~13 and 35%, respectively. Sixty-one percent or 450 of the 743 comparisons yielded disparities of < 20%.

A similar comparison (Figure 1b) was made against the GEMS/GLORI database. The problem of identifying consistent areas is likely to be greater here than with the UNESCO-based data since information has been drawn from several hundred independent literature sources. Nonetheless, the STN-30p and GEMS/GLORI data sets compare reasonably well. There were 314 from a total of 475 rivers which showed correspondence within 20% with an overall median of 11% and mean of 23%.

In both sets of comparisons, contributing basin areas below 25×10^3 km^2 show the poorest degree of agreement. This drainage area is likely to represent the practical limit of our ability to verify a 30-min network topology at the global scale. If basin areas below 25×10^3 km^2 are excluded from the analysis, the overall median and mean differences drop from 11-13% and 23-35% to ~6% and 16-18%, respectively, in both comparisons. At the same time, the proportion of areal estimates falling within ±20% increases substantially, from ~60-65% to 80% for both comparisons.

The lack of a perfect correspondence between STN-30p and previously published basin area estimates does not necessarily indicate an error in the simulated topology. Among published statistics given for individual basins in the GEMS/GLORI database itself are multiple entries for basin area which often differ substantially from one another. Several examples can be found in contrasting climatic zones, for all size classes of drainage basin, and at all levels of economic development (Table 1). Rivers smaller than 100×10^3 km^2 generally show the largest relative differences, many in excess of 100%. Large inconsistencies can be found even among what would be considered well-studied rivers in Europe and the United States (e.g., Thames, Seine, Dnestr, and Delaware). Basins with areas from 100×10^3 to 250×10^3 km^2 have less dramatic but nonetheless large ranges in reported areas that in many cases exceed 50%. As a general rule, the relative degree of agreement among independent estimates improves with increasing basin size, although disparities >50% exist among rivers with areas $>250 \times 10^3$ km^2.

The wide range in previously published estimates of drainage area arises in part from the acceptance and repetition of original, incorrect estimates. Disparities also arise from difficulties in delineating basin boundaries due to poor quality maps, complex and meandering drainage patterns, and/or the presence of engineered waterways. In addition, it is not always clear where the mouth of a river basin should be positioned when an elongated estuary or delta with multiple tributaries is encountered. There also is ambiguity about whether perennial, intermittent, or nondischarging portions of drainage systems are represented in the original data from which UNESCO/RivDIS and GEMS/GLORI have been compiled. Notable examples in Table 1 are the Orange, Rio Grande (United States), and Shatt el Arab basins. Outliers above the 1:1 lines in Figure 1 indicate the presence of such nondischarging (i.e., noncontributing) areas that are included in STN-30p but often are not tabulated in the original published sources.

Using reported area information from the Arctic region, we were able to minimize some of the difficulties otherwise encountered in the worldwide coverage represented by UNESCO/RivDIS and GEMS/GLORI. Figure 1c shows STN-30p in substantial agreement with previously reported values (median=3.3%,

Table 2a. Continental and Global-Scale Summaries of Total Land Mass Areas

Continent	STN-30p	Times Atlas†	*Korzoun et al.* [1978]	*Baumgartner and Reichel* [1977]
Africa	30.1	30.3	30.1	29.8
Antarctica	12.3	14.2	14.0	14.1
Asia	44.4	44.4	43.5	44.1
Australasia	8.2	8.9	8.9	8.9
Europe	10.2	10.6	10.5	10.0
North America	24.6	24.3	24.2	24.1
South America	17.9	17.8	17.8	17.9
Globe*	147.7	150.1	149.0	148.9

The spatial extent of each continent is defined in Figure 4a. The total land area is given in 10^6 km^2.

*Global totals for STN-30p do not include several small islands.

†*Bartholomew et al.* [1994, 1988].

Table 2b. Continental and Global-Scale Summaries of Glacierized and Nonglacierized Area

	STN-30p		*Korzoun et al.* [1978]		*Baumgartner and Reichel* [1977]	
Continent	Unglacierized	Glacierized†	Unglacierized	Glacierized	Unglacierized	Glacierized
Africa	30.1	0	30.1	0	29.8	0
Antarctica	0	12.3	0.1	14.0	0	14.1
Asia	44.4	0	43.3	0.2	44.1	0
Australasia	8.2	0	8.9	0	8.9	0
Europe	10.1	0.1	10.4	0.1	10.0	0
North America	22.4	2.2	22.2	2.0	22.4	1.7
South America	17.9	0	17.8	0	17.9	0
Globe*	133.1	14.6	132.8	16.2	133.1	15.8

The total area is given in 10^6 km^2.
*Global totals for STN-30p do not include several small islands.
†Glacierized areas in STN-30p bear no potential flow paths.

mean=4.8%, n=538). Contributing areas calculated in the STN-30p for 537 of 538 cases show <20% disparity. A total of 472 show <10% discrepancy. These statistics indicate that when high-quality data with standardized reporting procedures are employed, the STN-30p provides an accurate geographic description of drainage systems at 30-min spatial resolution down to ~10^4 km^2. This finding, together with careful examination and cross-referencing to map data at the global scale, suggests that apparent errors in basin area depicted by STN-30p can also reasonably represent errors and inconsistencies in the areas originally reported by UNESCO and GEMS/GLORI.

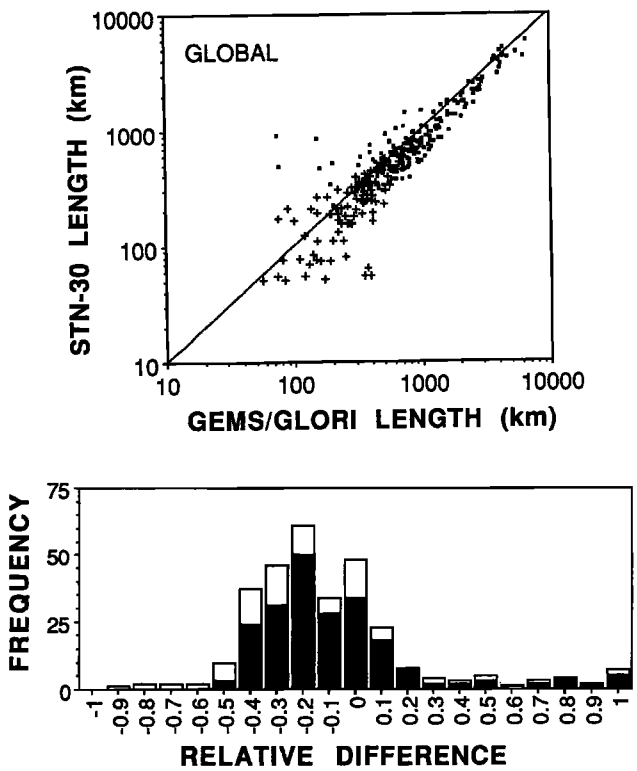

Figure 2. Maximum river (basin) lengths derived from STN-30p plotted against reported lengths from GEMS/GLORI (n=298) [*Meybeck and Ragu*, 1995, 1997]. Basins with area less than 25,000 km^2 are marked with crosses. The 1:1 line is also shown. Frequency distributions of relative difference are partitioned into basins above/below 25,000 km^2 (black/white portions of each histogram bar, respectively).

3.3.3. Total land mass comparison. In STN-30p, 90% (133 × 10^6 km^2) of the Earth's total land surface (148 × 10^6 km^2) is nonglacierized and capable of discharging runoff through river networks (Table 2a, b). This partitioning of the continental land mass by STN-30p can be compared to statistics given in earlier studies of global-scale hydrology [*Baumgartner and Reichel*, 1975; *Korzoun et al.*, 1978]. Total land area is similar among the three studies, and each compares well to independent atlas sources [e.g., *Bartholomew et al.*, 1994, 1988]. Aggregate areas of glacierized and nonglacierized land in STN-30p are generally within a few percent of the areas given by *Baumgartner and Reichel* [1975] and *Korzoun et al.* [1978] for both the globe and individual continents. The largest differences appear to be caused by alternative delineations of continental boundaries.

3.3.4. Basin length comparisons. A check was made of STN-30p maximum river lengths (based on the area-directed search algorithm described above) to corresponding entries in GEMS/GLORI. Although values for individual basins sometime differ greatly from previously cited values, maximum river lengths in STN-30p generally correspond well to the previously published values (Figure 2). Sixty percent or 178 of the 299 rivers compared show lengths within ±25%. Generally, STN-30p gives shorter river lengths compared to GEMS/GLORI. The computed slope of a linear regression between STN-30p and GEMS/GLORI reported lengths shown in Figure 2 is 0.89, suggesting a systematic and progressive underestimation with increasing river size. Median and mean differences are 16.0 and 11.4%, respectively, expressed as underestimates by STN-30p. The apparent disparity can be reduced by ~4% when maximum length is computed as the longest recorded STN-30p stream segment as opposed to the area-directed determination. STN-30p nonetheless records a general underestimate using either method.

Sinuosity contributes additional length that the STN-30p does not currently reflect and produces apparent underestimates relative to published sources. In areas known to be dominated by river meanders, the potential bias can be large. For example, in the Amazon River, STN-30p accounts for 70% of reported maximum length. Despite such disparity, suitable coefficients in river

Table 3. Mainstem Length Discrepancies in Extant Literature

River Basin	Country	Continent	Area STN-30p, 10^3 km^2	GEMS/GLORI Reported Length, Minimum, km	GEMS/GLORI Reported Length, Maximum, km	Range,* %	STN-30p Length, km
			>1000 km (from STN-30p)				
Amur	Russia	Asia	2902	2820	4352	43	5050 (1)
Yenisei	Russia	Asia	2582	3490	4129	17	4820 (1)
Mississippi	USA	North America	3203	3778	5985	45	4180 (1)
Huang He	China	Asia	894	4670	5465	16	4170
Parana	Argentina	South America	2661	4000	4700	16	3070 (1)
Ganges	India	Asia	1628	2525	5401	73	2220
Kolyma	Russia	Asia	666	2130	2599	20	2090
Orinoco	Venezuela	South America	1039	2061	2780	30	1970
Murray-Darling	Australia	Australasia	1032	2589	3490	30	1740 (1)
Volta	Ghana	Africa	398	1270	1600	23	1420
Brazos	USA	North America	125	1400	2060	38	1260
Negro	Argentina	South America	198	729	1000	31	1080 (1)
Fraser	Canada	North America	245	1110	1375	21	1070
			<1000 km				
Yana	Russia	Asia	235	872	1368	44	970
Mahanadi	India	Asia	141	851	1295	41	870
Ruvuma	Mozambique	Africa	154	640	800	22	830
Mobile	USA	North America	124	1064	1250	16	590
Sassandra	Ivory Coast	Africa	76.6	650	840	26	590
Douro	Portugal	Europe	97.1	772	925	18	570
Copper	USA	North America	67.2	360	460	24	510
Susitna	USA	North America	45.6	504	733	37	330
Konkoure	Guinea	Africa	15.2	260	365	34	290
Thames	Great Britain	Europe	17.3	336	405	19	270 (2)

The range in estimates of maximum river length is given below for several individual river systems as reported in the GEMS/GLORI data set [*Meybeck and Ragu*, 1995, 1997]. These examples represent a subset of all basins for which duplicate entries exist, ranked by STN-30p length. The numbers in parentheses offer likely reasons for the apparent disparities among reported lengths. (1) Headwaters not well defined. Longest branch may commonly be regarded as merely a tributary or as main river. In addition, several branches may have different names from that of river mouth. (2) Length depends on endpoint in estuarine zone.

*Although this computed range is calculated on the minimum and maximum reported lengths in GEMS/GLORI, the *Meybeck and Ragu* [1995, 1997] database does offer a preferred entry for each river. Range percent is computed here as $(\text{Maximum}_{\text{GLORI}} - \text{Minimum}_{\text{GLORI}})/\text{Mean}_{\text{GLORI}}$.

transport models have been developed to compensate for this underestimation [*Vörösmarty et al.*, 1989, 1991]. Further, it is unclear whether it is optimal to include river meanders in length estimates for river systems. It has been suggested instead that length along valley course might provide a better descriptive measure [*Dingman*, 1978].

STN-30p also yields overestimates of length compared to GEMS/GLORI. Since STN-30p is limited only by the topographic properties of individual basins, it will tabulate lengths even across nondischarging portions of a drainage basin. Thus, STN-30p typically will yield greater values for basin length compared to GEMS/GLORI, especially in dry regions, whenever GEMS/GLORI presents river length based on the area actively contributing runoff.

As with reported areas, differences in river length between GEMS/GLORI and STN-30p should be viewed in light of the several irregularities apparent in the literature from which the GEMS/GLORI database was developed (Table 3). Thus lengths reported in GEMS/GLORI can differ from one another because of the inconsistent inclusion of nondischarging areas (e.g., Amur River). Disparities also arise depending on whether named rivers or the physically longest river reaches are reported. For example, to define a length for the Mississippi basin, the Mississippi River source area (in the State of Minnesota) or the longest branch in the Missouri network could be used, but these estimates vary by more than 2000 km. A similar situation occurs for the Murray-Darling network with a nearly 1000 km difference. In addition, the published entries may reflect contrasting levels of sinuosity that are dependent on the resolution of original map sources which are difficult to establish.

4. Results and Discussion

In the following sections we present the principle drainage basin and river network characteristics of the STN-30p. The river networks are shown in Figure 3 and the drainage basin boundaries in Plate 1. We provide numerical summaries for each of six continents, the oceans, and the globe (Figure 4). We also offer information on the partitioning of the land mass into exorheic river systems with potential flow to the oceans as well as internal (endorheic) drainage basins. STN-30p network and drainage basin

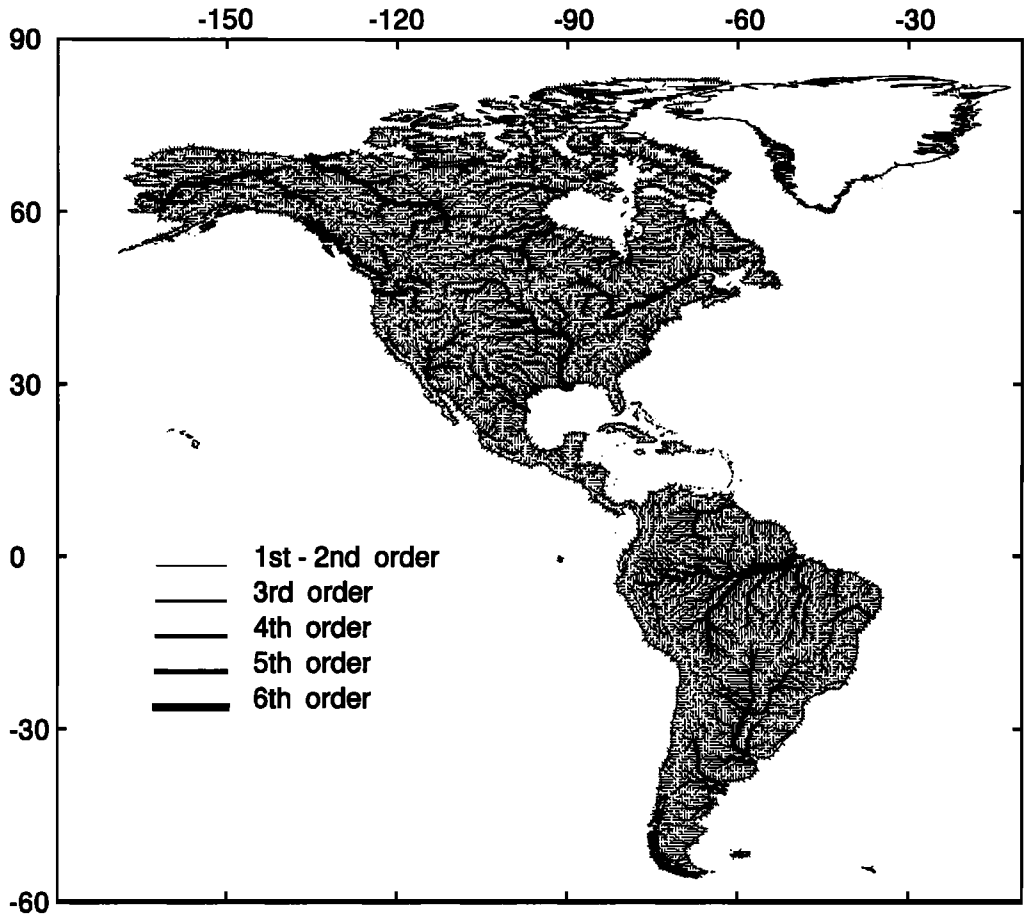

Figure 3. STN-30p, the Simulated Topological Network for potential river systems at 30-min (longitude × latitude) spatial resolution for (a) western and (b) eastern Hemispheres. Each of 59,132 land-based grid cells is assigned a direction of flow and linked to adjoining cells. Both exorheic and endorheic networks are represented in this data base. Order refers to individual river segments.

characteristics can be viewed from the standpoint of the continental land mass as well as of the oceans. We offer summaries based on both perspectives below.

4.1. Continental Perspective

4.1.1. Drainage basin numbers. There are 6152 individual watersheds represented in the STN-30p for the 133.1 × 10^6 km^2 of nonglacierized land area of the Earth. The total number of drainage basins declines rapidly as a function of river order at mouth (Table 4 [number of basins section]) over individual continents or the globe. The most common watershed (as classified by river order at mouth) is therefore order 1. Together with second-order basins, these smaller systems account for nearly 5800 individual STN-30p entries or 94% of all simulated watersheds. Globally, there are but 366 basins of order 3 or greater. More than 70% of these remaining systems are classified as order 3. Larger river systems are rare, with only 65 order 4 and 34 order 5 basins. The Amazon and Lena River systems represent the only order 6 basins at 30-min spatial resolution.

The total number of individual watersheds across a continent does not necessarily predict the relative abundance of particular basin orders. For example, despite its relatively small size, Australasia maintains 32 third-order basins, while the much larger land mass of South America shows but 21. While it is true that the fourth-, fifth-, and sixth-order river systems of South America contain a large number of third-order tributary basins, the entries in Table 4 (number of basins section) depict the connection of the land mass to potential receiving waters as tabulated at river mouths. By this measure, third-order basins in Australasia are more important in defining land-to-ocean linkages than in South America.

4.1.2. Drainage basin areas. Mean drainage basin area spans several orders of magnitude, from ~10^3 km^2 for first-order basins to >10^6 km^2 for orders 5 and 6 (Table 4 [mean basin area section]). Across the continents, mean basin area for order 3 rivers appears most consistent, varying by 20% or less around the global mean. For all other orders, larger proportional differences are evident and indicate that river order is a generally unreliable predictor of basin area. The greatest relative differences in continent-wide means are associated with order 5 (42-178% of the global mean).

For the entire Earth, there is a progressive increase in the total area drained by basins of order 1 through order 5-6 (Table 4 [aggregate basin area section]). Order 1 and 2 basins drain but 10

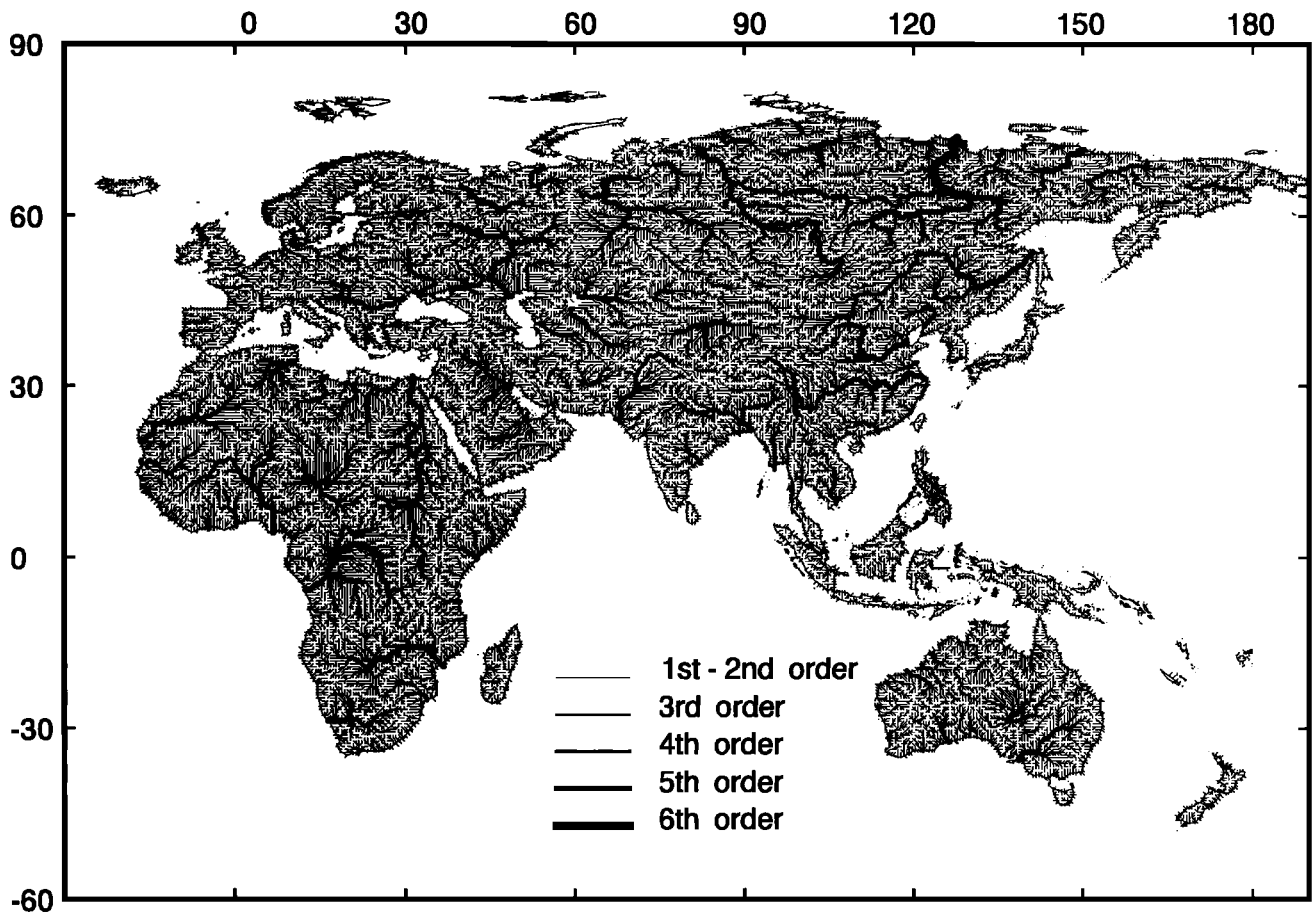

Figure 3. (continued)

and 15% of the land mass, respectively. Fifth- and sixth-order basins are quantitatively most important in terms of connecting land mass to receiving waters, and they alone drain nearly 45% of total area. This sequence of increasing area with order is more ambiguous for individual continents. In North America, for example, the lowest proportional contribution is associated with order 4 basins.

A log-log plot of cumulative land area drained versus basin rank (by area) yields an asymptotic curve for the globe (Figure 5). Basins ranked 23, 156, and 1123 drain areas of 10^6, 10^5, and 10^4 km^2, respectively. The largest 10, 100, and 1000 STN-30p potential rivers drain ~25, 65, and 90% of the land mass, respectively. About one-half of the terrestrial globe (53%) is potentially drained by the 50 largest STN-30p drainage basins and the remainder by more than 6100. Similarly skewed distributions are apparent for each of the continents (Figure 5). Globally, <1% of all STN-30p rivers drains 50% of the land mass, <5% drains 75%, and <25% drains 90%. The normalized distributions for individual continents resemble the global pattern with the exception of Australasia which requires a proportionally larger number of river systems to drain a fixed fraction of total land area.

4.1.3. Total length of ordered river segments. There is a global total of 3.24×10^6 km of STN-30p flow pathways that define the interior of the land mass at 30-min spatial resolution (Figure 3, Table 4 [total length of interior segments section]). The most dominant contribution to this total comes from lower-order river segments. Order 1 rivers are particularly important with $>2 \times 10^6$ km. High-order river segments are quantitatively less important. Order 5 and 6 rivers, for example, contribute fewer than 45×10^3 km or ~1% of the global total. This pattern also holds across orders for each of the six continents. Asia has the largest aggregate length (1.14×10^6 km) or 35% of the global total, reflecting its place as the largest continent. Africa and North America each have overall smaller total lengths that are nearly identical to each other (0.630×10^6 km). Europe and Australasia have the least aggregate length, 0.29 and 0.18×10^6 km, respectively.

4.1.4. Mean basin (mainstem) length. For the globe, the mean length of an STN-30p basin (i.e., length of mainstem) increases across sequential orders from less than 100 to greater than 4300 km (Table 4 [mean basin length section]). There is consistency among the continents for basin lengths associated with basin orders 1 through 3. Ranges in their means are approximately 70-110, 215-280, and 510-580 km, respectively. The mean lengths for basins of order 4 through 6 basins exceed 1000 km. Except for sixth-order rivers (n=2), the range for these large rivers across different continents is significant, from 984-1535 and 1378-3072 km for orders 4 and 5, respectively.

Each continent is more or less surrounded by a fringe of small to medium-sized basins at the land-ocean (or land-internal

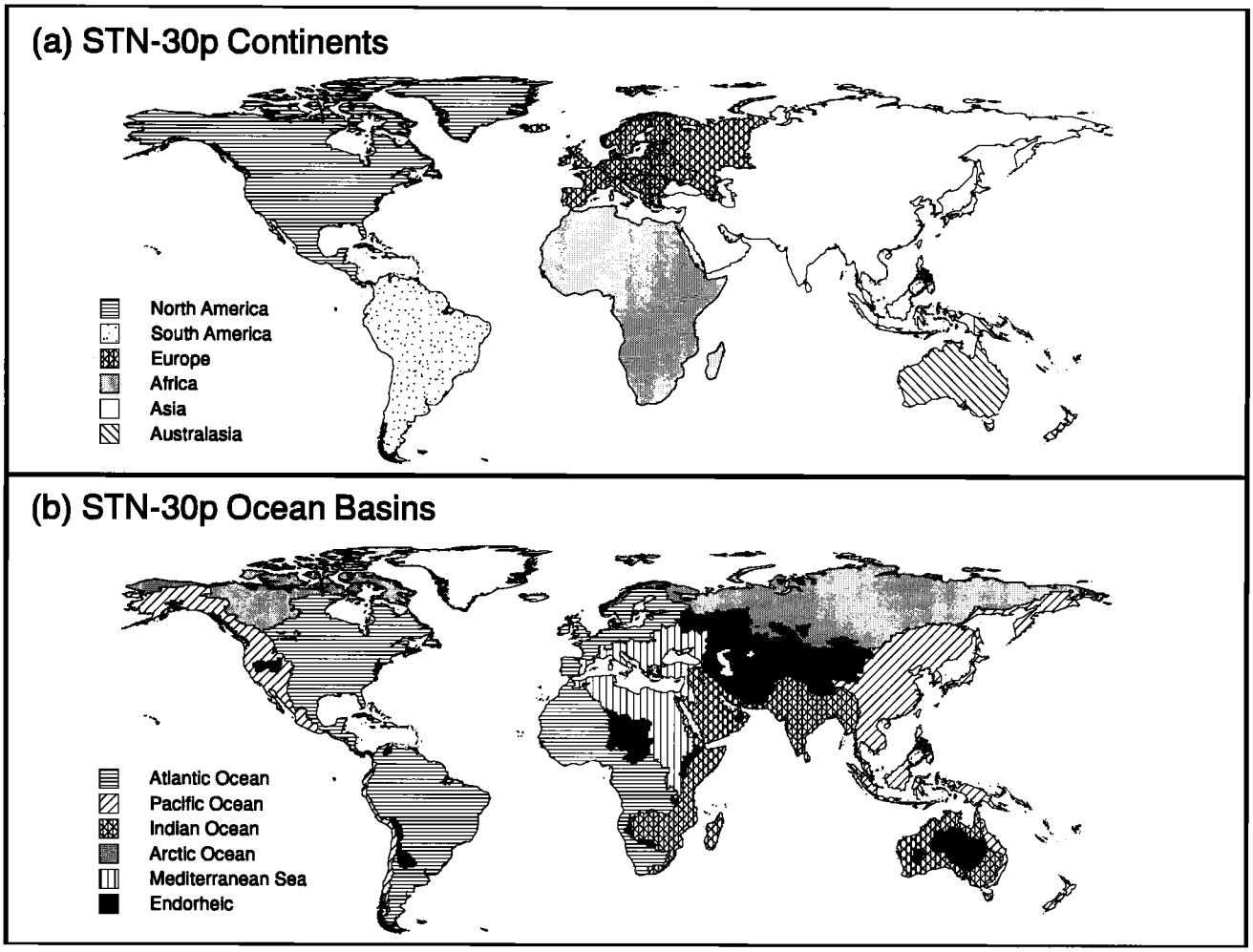

Figure 4. Division of STN-30p land mass into (a) individual continents and (b) inland and ocean drainage basins.

receiving body) interface (Plate 1). Large basins extend well into the continents and drain runoff often thousands of kilometers from basin outlets. The 50 largest river systems (ranked by area) all have mainstem lengths in excess of 1000 km and a mean of 2590 km. The remaining 6102 river basins show a mean of 137 km, and only about 40 have lengths exceeding 1000 km.

4.1.5. Summary for major river basins. As demonstrated above, large river systems drain a significant portion of individual continent and global land areas. Owing to their collective importance, we provide a listing of key drainage basin attributes for the 50 largest river basins (ranked by area) which together drain more than half of the Earth's land mass (Table 5). These attributes include physical information including exorheic/endorheic status, basin order, drainage area, basin length, and elevation at mouth. All such measures have been defined and discussed in preceding portions of the text. An additional 354 basins have been assigned names in the larger STN-30p data set.

4.2. Oceanic Perspective

4.2.1. Exorheic versus endorheic land mass. Of the total nonglacierized land mass in STN-30p (133×10^6 km^2), 87% (116×10^6 km^2) shows potential routing to the oceans (i.e., exorheic), while only 13% (17.4×10^6 km^2) is classified as internal drainage (endorheic) (Table 6a). Across individual continents, however, the relative importance of internal basins varies greatly. In Australasia and Asia, for example, endorheism is quantitatively very important in defining the character of the land mass. These continents have the greatest proportion of inland drainage areas, 28 and 20%, respectively (Table 6d). Europe also has a relatively high proportion of endorheic area (19%) owing to inclusion of the Volga basin which empties into the Caspian Sea. In contrast, North and South America are the most exorheic of all continents, with only 2 and 4% endorheic area, respectively.

4.2.2. Drainage basin area of each ocean. The STN-30p domain was reaggregated into five distinct drainage basins, each representing the potential contributing area to a major ocean (Figure 4b). The Atlantic Ocean has the largest such basin area with more than one-third of the global nonglacierized land mass or 45.6×10^6 km^2 (Table 6a). It contains the Amazon, together with nearly 1400 individual basins from order 1 through order 5 (Table 6b). Among the order 5 rivers are large continental basins such as the Mississippi, Zaire, and Parana. The Indian and Pacific basins have nearly identical contributing areas (21.1×10^6 km^2). Each occupies less than half the area of the Atlantic and individually drains 16% of total global land area. Both have rivers of order

Table 4. Continental and Global-Scale Summary of STN-30p River Basin Attributes

Order	Africa	Asia	Australasia	Europe	North America	South America	Global*
			Number of Basins				
1	326	1470	209	621	1591	331	4663
2	152	355	74	138	302	94	1123
3	39	86	32	33	54	21	265
4	10	27	5	5	9	9	65
5	9	11	2	4	7	1	34
6	–	1	–	–	–	1	2
Total	536	1950	322	801	1963	457	6152
			Mean Basin Area (10^3 km^2)				
1	5.0	3.1	4.5	2.4	2.1	4.4	3.0
2	20.2	15.6	17.9	13.9	12.8	21.7	16.0
3	81.8	78.3	79.7	64.7	58.3	81.1	73.4
4	444	336	191	400	270	464	355
5	1970	1460	1000	634	1370	2660	1490
6	–	2420	–	–	–	5850	4140
			Aggregate Basin Area (10^6 km^2)				
1	1.63	4.61	0.95	1.50	3.32	1.45	13.8
2	3.06	5.55	1.32	1.92	3.86	2.04	17.8
3	3.19	6.73	2.55	2.13	3.15	1.70	19.5
4	4.44	9.06	0.95	2.00	2.43	4.18	23.1
5	17.7	16.0	2.01	2.54	9.61	2.66	50.6
6	–	2.42	–	–	–	5.85	8.3
Total	30.1	44.4	7.8	10.1	22.4	17.9	133.1
			Total Length of Interior Segments (10^3 km)				
1	405	771	126	203	447	238	2190
2	140	224	37.2	57.5	115	79.2	653
3	54.7	89.6	14.3	18.8	39.8	31.7	249
4	20.7	36.8	3.8	6.5	15.0	15.2	98.0
5	12.4	13.9	0.5	2.9	9.1	2.6	42.2
6	–	1.4	–	–	–	1.0	2.4
Total	633	1140	182	289	626	368	3240
			Mean Basin Length (km)†				
1	107	80.2	98.4	75.7	71.5	95.0	80.2
2	260	227	220	221	214	278	231
3	584	553	554	531	512	580	549
4	1316	1290	984	1372	1188	1535	1296
5	2846	2951	1378	1630	2767	3072	2641
6	–	4387	–	–	–	4327	4357

Statistics correspond to river systems defined by the order of each mainstem at river mouth. The spatial extent of each continent is defined in Figure 4a.

*Global totals incorporate the statistics for several small islands.

†On the basis of mainstem length determined by area-directed upstream search.

1 through 5 with a total of ~800 individual basins for the Indian Ocean and 1560 for the Pacific. Large Pacific river basins include the Amur, Changjiang, Columbia, and Mekong, all order 5 except for the Mekong (order 4). Examples of large Indian Ocean basins include the order 5 Zambezi, Ganges, Indus, and Murray Rivers. The Arctic has the next largest cumulative basin area with 17.0×10^6 km^2 or 13% of the nonglacierized land mass. More than 1600 individual basins exist with orders 1 through 6. Order 5-6 river systems (i.e., Lena, Ob, Yenisei, and Mackenzie) dominate the cumulative Arctic land area drained. The Mediterranean/Black Sea has the smallest basin area with 10.9×10^6 km^2 or <10% of the global land mass. Basin orders are from 1 through 5. There are several large contributing rivers including the order 5 Nile, arheic Irharhar, and Don as well as the order 4 Danube and Dnepr. There are 450 internally draining basins from order 1 through 5. Large endorheic rivers of order 5 include the Chari, Volga, and Syr-Darya.

Table 6c repartitions each continent's land area to individual ocean basins as well as to its endorheic receiving bodies. Table 6d summarizes these numbers in terms of percentages. Each continent

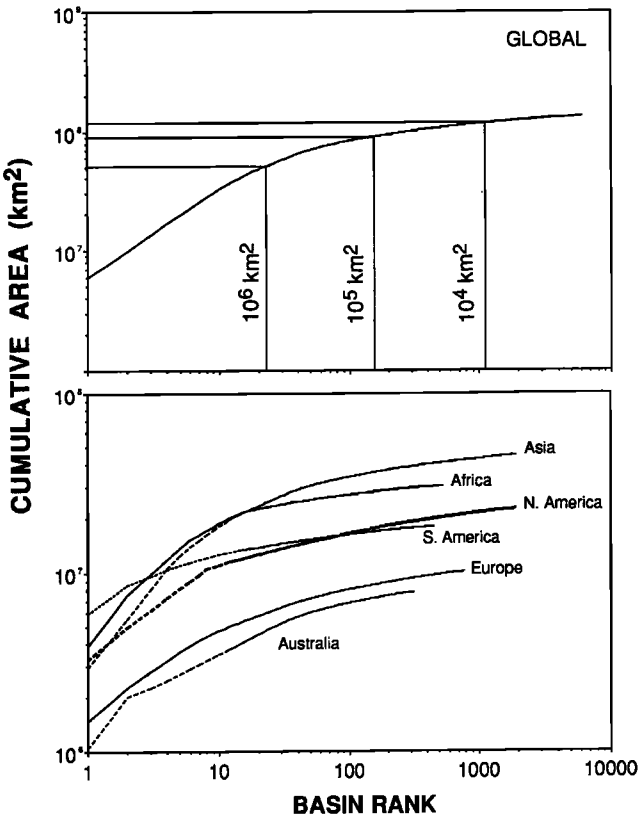

Figure 5. Accumulated area drained expressed as a function of river basin rank for the globe and for individual continents. Rank is based on drainage basin area at mouth for individual river systems. The vertical lines show rank at which indicated basin size is attained.

can potentially contribute runoff to at least two and up to four individual oceans plus endorheic basins (Figure 4b). South America has a STN-30p basin area associated with both the Atlantic and the Pacific but owing to the position of the Andes along its western coast has more than 10 times its area contributing to the Atlantic than to the Pacific (89 versus 7%). Australasia shows a similar skewness with more than 4 times the land area directed toward the Indian Ocean than to the Pacific (58 versus 14%). Land area in Africa, Europe, and North America is assigned to three oceans. For Africa, nearly half of all land area potentially flows to the Atlantic while 20-25% flows to the Indian Ocean and Mediterranean/Black Sea. About equal proportions of land area in Europe (30-35%) flow into the Atlantic and Mediterranean, while only 15% is directed to the Arctic Ocean. For North America, more than half of all land area flows potentially to the Atlantic while ~20% each flows to the Pacific and Arctic Oceans. Asian land mass is linked to four oceans. Over 30% of its land area is assigned to the Pacific and 20-25% to the Arctic and Indian Oceans. It also provides a very small proportion to the Mediterranean in the region of the Middle East.

Table 6c can also be viewed from the standpoint of potential continental source areas draining to individual oceans. Table 6e offers a summary of the relative contribution of each continent's land mass to the total contributing area possible for each ocean basin. Each ocean is associated with land mass from either three or four continents. The Arctic Ocean receives two-thirds of its potential contributing land area from Asia, one-quarter from North America and the remainder from Europe. The Atlantic receives roughly equivalent basin area from Africa and North and South America (28-35% each) and <10% from Europe. The Indian Ocean gets roughly one-half of its area from Asia, one-third from Africa, and the rest from Australasia. Land area connected to the Mediterranean/Black Sea is dominated by Africa (65%). Europe (28%) and Asia (7%) play relatively minor roles. The Pacific shows about two-thirds of its basin area derived from Asia and one-quarter from North America. It receives 6% each from Australasia and South America, reflecting the presence of the mountain chains positioned inland a short distance and parallel to the coastlines of each continent (i.e., Great Dividing Range in Australia and Andes in South America). A more complete view of these land-ocean connections must also include the spatial distribution of runoff and discharge under particular climatic regimes which change over time. STN-30p provides the maximum potential contributing areas.

4.2.3. Fluvial distance and travel time to basin outlet. We define the distance water moves along STN-30p flow pathways as fluvial distance. The cumulative distribution of land area as a function of fluvial distance to basin outlet shows that most of the global land mass is positioned well upstream of river mouths (Figure 6). Only 10% of the total nonglacierized land mass is within 100 km of a coastline, and only 25% is within 250 km. Exactly one-half of the land is within 750 km, and 57% is 1000 km or closer to a river mouth. Twenty-five percent of the land mass is positioned more than 1700 km from an exorheic or endorheic endpoint. Distances longer than 2500 km are relatively infrequent, accounting for 12% of all STN-30p land area. Only 7% of the land mass is at 3000 km, and 2% is at 4000 km upstream of a river mouth. Such asymptotic distributions also characterize the individual continents (Figure 6).

Distances to river mouth inside STN-30p basins vary from <100 km for several thousand small coastal river basins to almost 6000 km for the world's longest river, the Nile. A map of such distances along all STN-30p directed line segments (Figure 7) shows the manner in which the potential river network penetrates the continental land mass. There are 6152 cells representing STN-30p river mouths. Among these, a large number (n=5702) represents coastal grid cells that are immediately adjacent to an ocean and which serve as the perimeter for each continent (Plate 1). The remainder (n=450) are endpoints of endorheic drainage basins linked to inland receiving bodies.

Across all STN-30p flow pathways, the global mean travel distance to river mouth is 1050 km with individual continental values varying from 460 to 1340 km (Table 6f). Australasia has the shortest mean upstream distance, while Africa has the longest. South America and Asia also have long travel distances owing to the presence of large high-order river systems. Distances tabulated by ocean basin show a range in means from 700 to 1400 km. The Indian Ocean has the shortest connection to the land mass with 740 km. This mean distance is comparable to the 690 km tabulated for endorheic basins. The longest mean distance is for the Mediterranean, demonstrating the large impact of the Nile River (mainstem length 5910 km).

Using STN-30p distances, we can make a simple calculation of mean travel time for runoff draining the continents. Assuming a uniform channel velocity of 0.5 m s^{-1} [*Vörösmarty et al.*, 1996a, 1991, 1989; *Liston et al.*, 1994; *Naden*, 1993] and neglecting lakes,

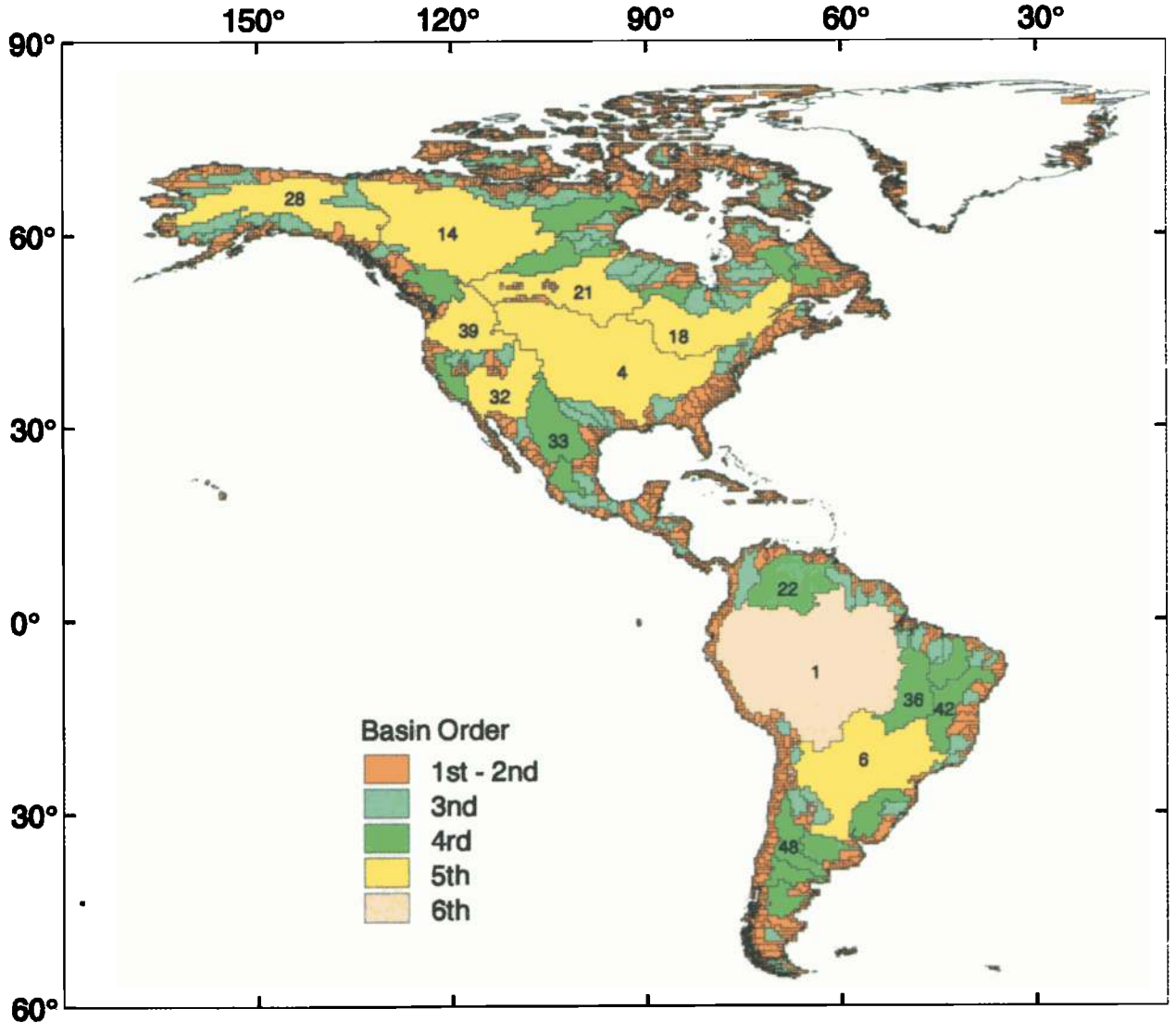

Plate 1a. Drainage basin boundaries defined by river systems within the STN-30p. For the globe, there are 6152 individual watersheds with 2420 in the Western Hemisphere. Order refers to basin order defined by river segment at mouth. White cells within the continents represent endpoints of endorheic drainage basins. Glacierized regions are also shown in white.

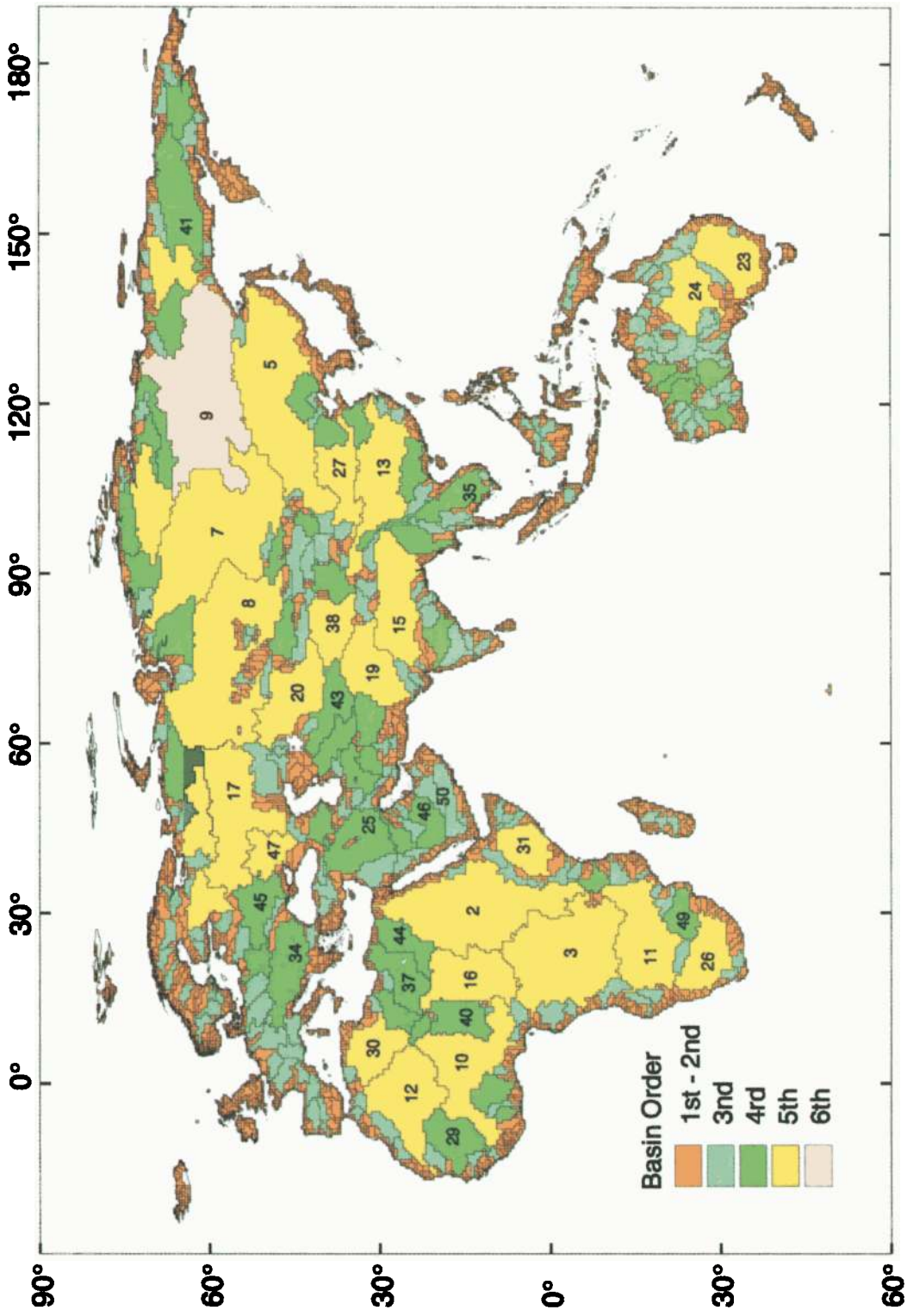

Plate 1b. Same as for Plate 1a, but for the Eastern Hemisphere with 3732 individual watersheds.

Table 5. Characteristics of the 50 Largest River Systems of the World Ranked by Area in STN-30p

Rank	Name	Continent†	Ocean‡	Order	Potential Basin Area, 10^6 km^2	Length, km	Elevation of Mouth, m
1	Amazon	SAM	ATL	6	5.854	4327	0
2	Nile	AFR	MED	5	3.826	5909	0
3	Zaire	AFR	ATL	5	3.699	4339	0
4	Mississippi	NAM	ATL	5	3.203	4185	0
5	Amur	ASIA	PAC	5	2.903	5061	0
6	Parana	SAM	ATL	5	2.661	2748	0
7	Yenisei	ASIA	ARC	5	2.582	4803	0
8	Ob	ASIA	ARC	5	2.570	3977	0
9	Lena	ASIA	ARC	6	2.418	4387	0
10	Niger	AFR	ATL	5	2.240	3401	0
11	Zambezi	AFR	IND	5	1.989.	2541	0
12	Tamanrasett*	AFR	ATL	5	1.819	2777	0
13	Chang Jiang	ASIA	PAC	5	1.794	4734	0
14	Mackenzie	NAM	ARC	5	1.713	3679	0
15	Ganges	ASIA	IND	5	1.628	2221	0
16	Chari	AFR	Endorheic	5	1.572	1733	260
17	Volga	EUR	Endorheic	5	1.463	2785	-40
18	St. Lawrence	NAM	ATL	5	1.267	3175	0
19	Indus	ASIA	IND	5	1.143	2382	0
20	Syr-Darya	ASIA	Endorheic	5	1.070	1615	40
21	Nelson	NAM	ATL	5	1.047	2045	0
22	Orinoco	SAM	ATL	4	1.039	1970	0
23	Murray	AUST	IND	5	1.032	1767	0
24	Great Artesian Basin	AUST	Endorheic	5	0.978	1045	70
25	Shatt el Arab	ASIA	IND	4	0.967	2200	0
26	Orange	AFR	ATL	5	0.944	1840	0
27	Huang He	ASIA	PAC	5	0.894	4168	0
28	Yukon	NAM	PAC	5	0.852	2716	0
29	Senegal	AFR	ATL	4	0.847	1680	0
30	Irharhar*	AFR	MED	5	0.842	1482	0
31	Jubba	AFR	IND	5	0.816	1699	0
32	Colorado (United States)	NAM	PAC	5	0.808	1808	0
33	Rio Grande (United States)	NAM	ATL	4	0.805	2219	0
34	Danube	EUR	MED	4	0.788	2222	0
35	Mekong	ASIA	PAC	4	0.774	3977	0
36	Tocantins	SAM	ATL	4	0.769	2234	0
37	Araye*	AFR	MED	4	0.742	1682	0
38	Tarim	ASIA	Endorheic	5	0.733	1227	840
39	Columbia	NAM	PAC	5	0.724	1791	0
40	Tafassasset*	AFR	Endorheic	4	0.686	1529	260
41	Kolyma	ASIA	ARC	4	0.666	2091	0
42	Sao Francisco	SAM	ATL	4	0.615	2212	0
43	Amu-Darya	ASIA	Endorheic	4	0.612	1976	40
44	Qattara*	AFR	MED	4	0.582	1903	0
45	Dnepr	EUR	MED	4	0.509	1544	0
46	Dawasir*	ASIA	IND	4	0.474	1435	0
47	Don	EUR	MED	5	0.423	1401	0
48	Colorado (Argentina)	SAM	ATL	4	0.422	1750	0
49	Limpopo	AFR	IND	4	0.420	1316	0
50	Muqshin*	ASIA	IND	3	0.414	1586	0

These rivers collectively drain 53% of the continental land mass. Statistics are defined and described in the text. For locations, see Plate 1.

*River system mostly nondischarging under present climate

†AFR, Africa; AUST, Australasia; EUR, Europe; NAM, North America; SAM, South America. See Figure 4a.

‡ATL, Atlantic Ocean; ARC, Arctic Ocean; IND, Indian Ocean; MED, Mediterranean/Black Sea; PAC, Pacific Ocean. See Figure 4b.

reservoirs, and wetlands, the mean travel times for the 50 largest basins from headwater to mouth would be of the order of 60 days, in contrast to 3 days for the remaining watersheds (see section 4.1.4). Such differences are important not only in defining the hydrologic responsiveness of river systems [*Dingman*, 1994; *Beven and Wood*, 1993; *Naden*, 1993; *Kirkby*, 1976; *Leopold et al.*, 1964; *Horton*, 1945] but as well the transport and processing of dissolved and particulate constituents [*Billen et al.*, 1994; *Milliman and Syvitski*, 1992]. If we assume a 10% underestimate in length due to meanders (section 3.3.4), a global mean travel time for runoff over all STN-30p river channels, again neglecting lakes, reservoirs or wetlands is 26 days, in substantial agreement with the 16 days proposed by *Covich* [1993]. Recent work [*Vörösmarty et al.*, 1997b, c] has demonstrated the

Table 6a. Areal Attributes of Potential Contributing Basins

Ocean/ Receiving Body	Total Land Area, 10^6 km^2	Fraction of Land Area, %	Ocean Area, 10^6 km^2	Land:Ocean Area Ratio
Arctic	17.0	13	14.1	1.21
Atlantic	45.6	34	82.5	0.55
Indian	21.1	16	73.4	0.29
Mediterranean*	10.9	8	2.5	4.36
Pacific	21.1	16	166.2	0.13
Internal	17.4	13	–	–

Land mass area contributed by STN-30p river systems to individual ocean basins and internal receiving bodies are tabulated here and in remaining portion of Table 6. The partitioning applies to all non-glaciated land area. Land mass division is shown in Figure 4.
*Includes Black Sea

Table 6b. Distribution of Orders for Potential Contributing Basins

Ocean/ Receiving Body	Order						TOTAL
	1	2	3	4	5	6	
Arctic	1373	227	29	8	6	1	1644
Atlantic	996	278	84	19	9	1	1387
Indian	568	172	54	12	5	–	811
Mediterranean*	228	56	13	5	3	–	305
Pacific	1242	267	31	9	6	–	1555
Internal	256	123	54	12	5	–	450

Entries are number of basins.
*Includes Black Sea

Table 6c. Land Area Contributed by Individual Continents to Oceans and Endorheic Receiving Bodies

Ocean/ Receiving Body	Africa	Asia	Australasia	Europe	North America	South America
Arctic	–	11.2	–	1.55	4.22	–
Atlantic	13.4	–	–	3.56	12.6	16.0
Indian	6.46	9.91	4.75	–	–	–
Mediterranean*	7.06	0.81	–	3.05	–	–
Pacific	–	13.6	1.16	–	5.06	1.22
Internal	3.14	8.85	2.28	1.93	0.55	0.63
Total	30.1	44.4	8.19	10.1	22.4	17.9

Entries are in units of 10^6 km^2.
*Includes Black Sea.

Table 6d. Proportion of Land Area from Each Continent Distributed to Individual Oceans and Endorheic Basins

Ocean/ Receiving Body	Africa	Asia	Australasia	Europe	North America	South America
Arctic	–	25	–	15	19	–
Atlantic	45	–	–	35	56	89
Indian	21	22	58	–	–	–
Mediterranean*	24	2	–	30	–	–
Pacific	–	31	14	–	23	7
Internal	10	20	28	19	2	4
Total	100	100	100	100	100	100

Individual entries represent % of each continent's land mass.
*Includes Black Sea.

Table 6e. Relative Contribution of Individual Continents to Total Contributing Drainage Basin Areas for Individual Oceans and Endorheic Basins

Ocean/ Receiving Body	Africa	Asia	Australasia	Europe	North America	South America	Total
Arctic	–	66	–	9	25	–	100
Atlantic	29	–	–	8	28	35	100
Indian	31	47	22	–	–	–	100
Mediterranean*	65	7	–	28	–	–	100
Pacific	–	64	6	–	24	6	100
Internal	18	51	13	11	3	4	100

Individual entries represent % of each receiving body's entire potential drainage system.
*Includes Black Sea

Table 6f. Mean Distance to Ocean for Individual Continents and Ocean Basins

Ocean/ Receiving Body	Africa	Asia	Australasia	Europe	North America	South America	Ocean Mean
Arctic	–	1500	–	402	716	–	1170
Atlantic	1380	–	–	304	1030	1429	1160
Indian	823	796	504	–	–	–	736
Mediterranean*	1970	329	–	695	–	–	1410
Pacific	–	1240	169	–	793	134	1010
Internal	753	528	529	1579	180	253	691
Continent Mean	1340	1120	461	655	867	1290	1050

Entries are in kilometers.
*Includes Black Sea

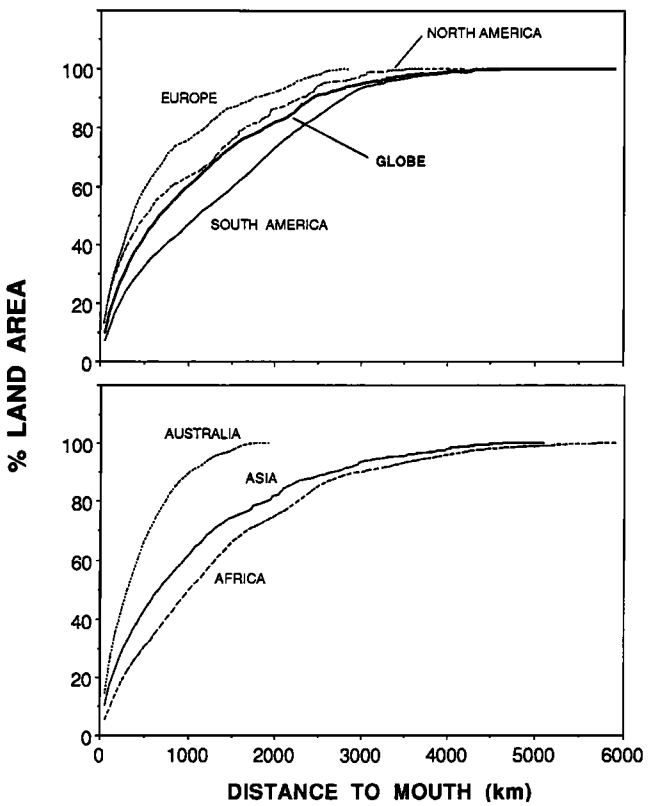

Figure 6. Cumulative land area and corresponding distances from river mouth along all STN-30p flow paths for the globe and individual continents. Distance was computed as the mean of all grid cells positioned the same distance upstream from river mouth (measured in units of whole grid cells).

presence of significant delays in continental runoff due to passage through run-of-river reservoirs. The travel times estimated above therefore apply to conditions prior to widespread impoundment of global river systems [see also *Dynesius and Nilsson*, 1994].

4.3. Reconciling Continental and Oceanic Perspectives

The organization of the Earth's land mass by STN-30p into large river systems has an important effect on the manner in which remote landscape units are connected to inland and coastal receiving waters. Although large watersheds of orders 3 through 6 are less prominent in terms of frequency (366 out of the global total of 6152), they drain the largest proportion of continental land mass, 102×10^6 km^2 or 76% of the total nonglacierized land mass (Table 4 [number of basins and aggregate basin area sections]). In STN-30p the land mass is divided into 59,132 individual grid cells. These are grouped into more than 33,000 interior river segments, each defined by a contiguous set of equal-ordered grid cells. If the total area occupied by each gridded river segment is summed by order, it is easy to demonstrate that order 1 river segments are quantitatively most important, with an exponential decline thereafter across all remaining orders (Figure 8a). Although >65% of the world's land area is potentially drained by these order 1 segments, only 10% is expressed as a direct connection to receiving waters. The bulk of this accumulated low-order drainage area is captured within larger river systems. For this reason, when moving from basin (mouth) order 1 through 5, we see a progressive increase in the proportion of land mass drained (Figure 8b), with order 5 basins collectively most important. Including the area represented by the two order 6 rivers accentuates this effect.

From a continental perspective, small order rivers therefore dominate the continental land mass and provide the most common

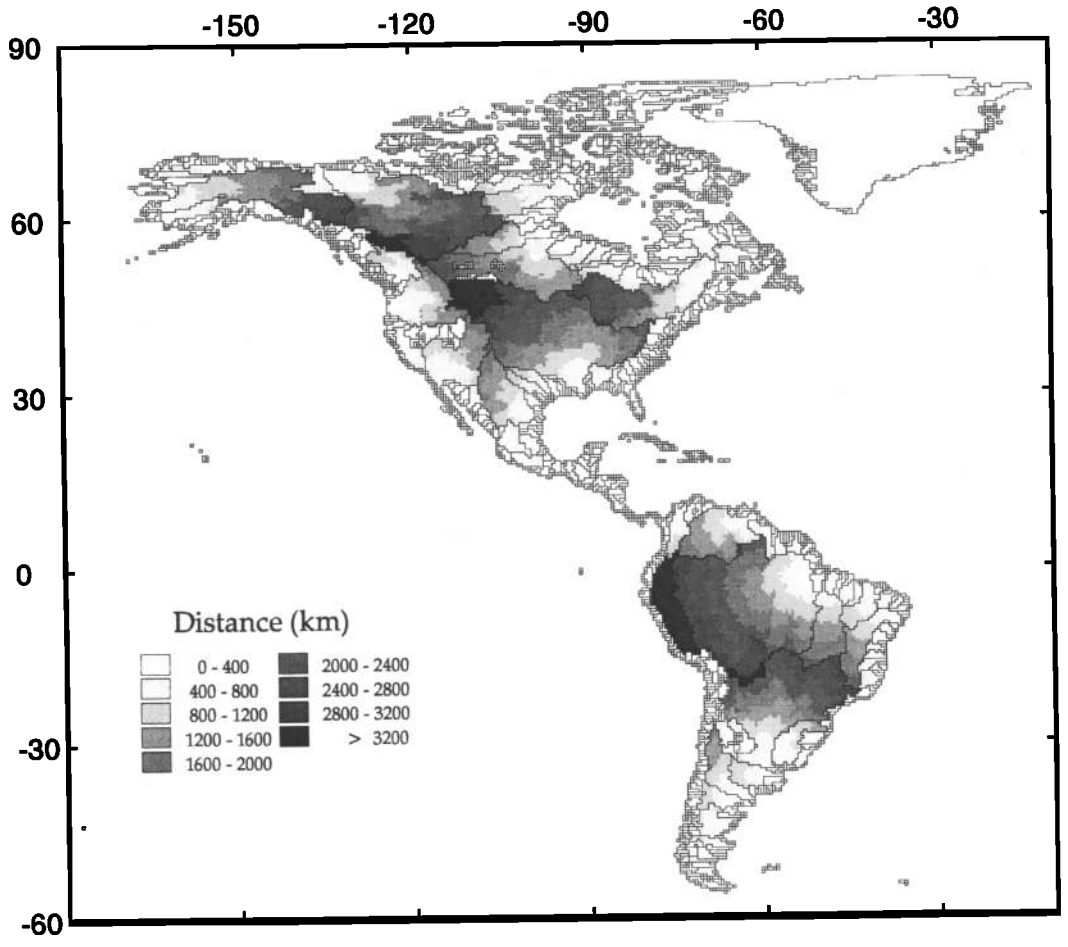

Figure 7. Spatial distribution of distance from river mouth along all STN-30p flow paths (fluvial distance to basin outlet) for (a) Western and (b) Eastern Hemispheres.

landscape for the generation and transport of water and constituents From an oceanic perspective, however, river mouths reveal to the world's coastal zones a contributing land mass area that is expressed fundamentally through larger-order river basins, most notably order 5 plus 6 in STN-30p.

The ratio of land-to-ocean area is one measure of the potential impact of continental runoff on individual ocean basins (Table 6a). This index varies greatly for different oceans. Two ocean basins have contributing land areas greater than those of the oceans themselves. The relatively enclosed Mediterranean/Black Sea shows a value of 4.4, reflecting a large aggregate area of dry river basins in North Africa. The Arctic Ocean and its associated land mass yield a ratio of 1.2. The remaining oceans show much smaller relative contributions from land. For the Atlantic, land area is about one-half of the corresponding ocean area. The land drainage of the Indian Ocean represents ~30% of its ocean area. The Pacific Ocean has the smallest proportion of contributing land area, representing only ~15% of total oceanic surface area.

5. Conclusions

We have analyzed the spatial organization of the global land mass using a simulated topological network (STN-30p) representing potential flow pathways across the entire nonglacierized surface of the Earth at 30-min (longitude × latitude) spatial resolution. We have described in detail the procedures used to develop this topology and to verify it. Using STN-30p, we derived a set of numerical attributes describing individual drainage basins, continents, ocean basins, and the globe.

STN-30p was developed expressly to support a range of Earth systems studies which require digital river basin information at or close to 30-min spatial resolution. Spatially distributed runoff fields from macroscale water balance models [e.g., J.B. Holden et al., A permafrost-based water balance model, submitted to *Arctic and Alpine Research*, 2000; *Arnell*, 1995; *Vörösmarty et al.*, 1998b, 1996a, 1991, 1989; *Mintz and Serafini*, 1989] and/or climate simulations [e.g., *Kite et al.*, 1994; *Sausen and Dümenil*, 1994; *Miller and Russell*, 1992], when linked to topologically organized river systems, provide a mechanism to validate model outputs by using well-established, station-based records of river discharge. The organization of water budgets through drainage basins and river systems as well can provide support to broad-scale impact assessments of climate change [*Arnell et al.*, 1996, *Kaczmarek et al.*, 1996] and water resource use [*Shiklomanov*, 1997, *Postel et al.*, 1996, *L'vovich and White*, 1990] on the terrestrial water cycle. The 1° to 30-min scale is also developing as the focal point for continental and global-scale constituent transport modeling [e g , *Seitzinger and Kroeze*, 1998,

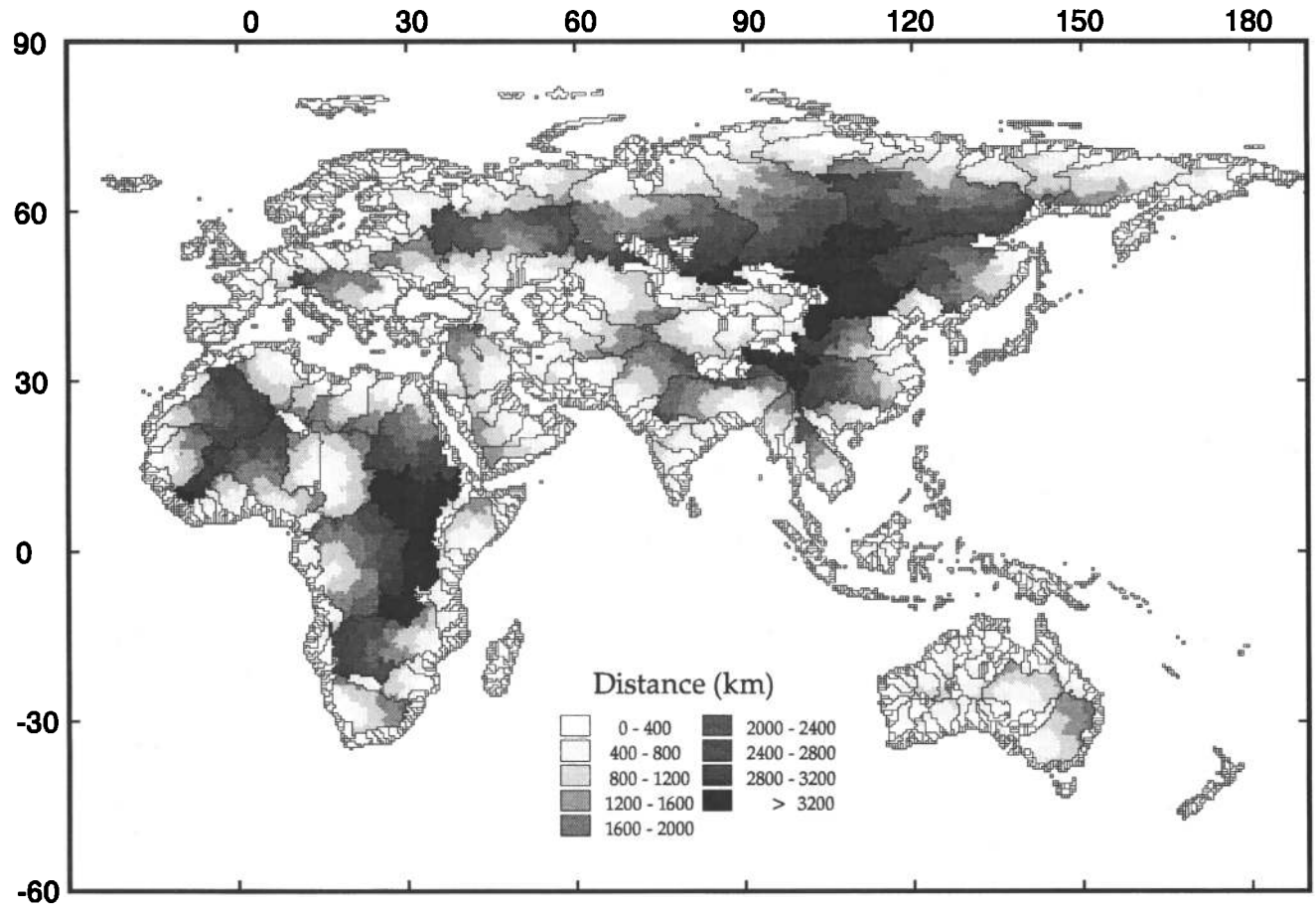

Figure 7. (continued)

Ludwig et al., 1996a, b; *Vörösmarty et al.*, 1997a; *Esser and Kohlmaier*, 1991] which will require simulated river networks like STN-30p. Knowledge of the organization of river systems also is important to the design and execution of river monitoring programs, particularly in the context of deriving continental and global-scale river fluxes for water and constituents [*Meybeck and Ragu*, 1997; *Vörösmarty et al.*, 1997a; *Grabs et al.*, 1996].

We have adopted the notion of a topographically controlled river networking system throughout this paper, and the description of rivers at the global scale refers to the set of both flowing rivers and nonflowing rivers under contemporary climate. Except for the large endorheic depressions, the entire set of flow pathways at 30-min spatial resolution represents a potential river networking system for the entire land mass of the Earth. In this way, the potential river networking in STN-30p provides a flexible framework for large-scale modeling studies. For example, STN-30p can be used in conjunction with general circulation model (GCM) climate change scenarios to simulate the reestablishment of discharge to the ocean from a currently arid region should a sustained increase in precipitation (and hence runoff) be predicted to occur.

STN-30p has limitations which we highlighted throughout the text. We have highest confidence in the depiction by STN-30p of large river systems (> 25,000 km^2). We also believe that composite statistics of river systems are generally sound across all size classes when expressed at continental, ocean basin, and global scales. We have relatively less confidence in the representation of individual drainage basins smaller than 25,000 km^2 using a 30-min grid resolution. For such basins, network attributes like mainstem length should therefore be viewed with due caution. Nonetheless, our levels of confidence must also be considered from the standpoint of the quality of previously published data that are relied upon for network verification, which themselves introduce a significant level of uncertainty. As discussed earlier, it may well be that STN-30p represents drainage basin characteristics with equal or improved fidelity. At the minimum, the standardized procedures used to develop STN-30p have helped to clarify apparent ambiguities in key drainage basin attributes such as mainstem length and endorheic versus exorheic drainage area Digital river networks such as the STN-30p afford scientists the opportunity to reduce this ambiguity in existing geomorphometric definitions by providing consistent and reproducible measures of drainage basin attributes.

Presumably, many of the limitations inherent within a 30-min topology will be substantially reduced with the advent of high-resolution 1-km global elevation models and river networks (see HYDRO1K: Elevation derivative database available at http://edcwww.cr.usgs.gov/landdaac/gtopo30/hydro/index.html and Global 30-arc second elevation date set available at http://edcwww.cr.usgs.gov/landdaac/gtopo30/README.html) We have developed an algorithm to aggregate 1-km flow pathways to

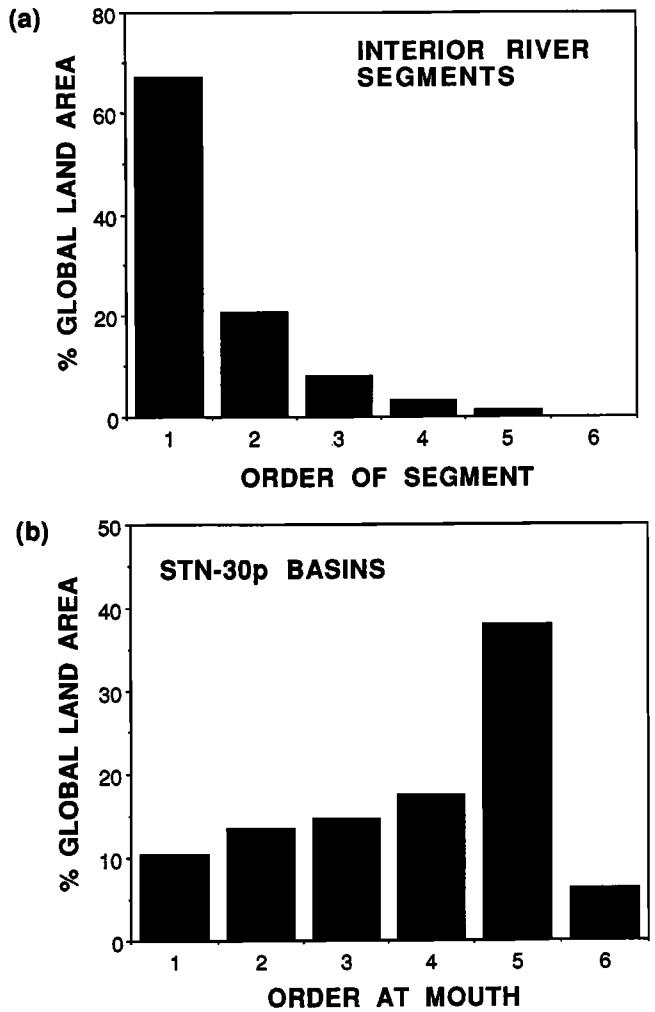

Figure 8. The relative contribution of 30-min resolution grid-cell areas depicting the land mass of the Earth by different river orders: (a) area drained by all interior river segments classified by river order (Figure 3) and (b) accumulated area for all drainage basins classified by order at river mouth (Plate 1). Figure 8a demonstrates how smaller-order river segments are distributed across the land surface of the Earth from a continental perspective. Note the predominance of order one segments. Figure 8b reflects an oceanic perspective in which the linkage of the land mass to coastal and inland receiving waters is dominated collectively by order 5 and 6 river systems.

multiple scales [B. Fekete et al., Scaling gridded river network for macro-scale hydrological applications, submitted to *Hydrological Processes*, 2000] which will help reduce the limitations of a 30-min data set in depicting small drainage basins. Nonetheless, there are distinct advantages to using the STN-30p operating at 30-min spatial resolution. First, it has been geographically coregistered to both the UNESCO/RivDIS [*Vörösmarty et al.*, 1998a, 1996b] and GEMS/GLORI [*Meybeck and Ragu*, 1997, 1995] data banks to facilitate calibration and validation of drainage basin models for both water and constituents. Second, its computational burden and disk storage requirements are modest compared to a 1-km topology, especially when considering continental-to-global scale applications.

We offer free and unrestricted access to the STN-30p to all interested parties who contact us at the corresponding address or through http://www.watsys.unh.edu/.

Acknowledgments. We wish to thank our colleagues who helped to verify the STN-30p digital products (S. Kempe, University of Darmstadt, Germany; N. Fleming, CSIRO Division of Water Resources, Canberra, Australia; R. Wasson, Australian National University, Canberra, Australia). Assistance was provided by S. Glidden and B. Tucker on database development and graphics. Financial support to develop this data set came from the NASA Earth Observing System (NAG5-6137), NSF Division of Atmospheric Sciences (ATM-9707953), Office of Polar Programs (OPP-9524740), NASA-Tropical Rainfall Monitoring Mission (NAG5-4785), and the Department of Energy (DE-FG02-92ER61473).

References

Arnell, N.W., Grid mapping of river discharge, *J. Hydrol., 167*, 39-56, 1995.

Arnell, N., et al., Hydrology and freshwater ecology, in *Climate Change 1995: Impacts, Adaptations, and Mitigation of Climate Change*, edited by R.T. Watson, et al., Chap. 10, Cambridge Univ. Press, New York, 1996.

Band, L.E., and I.D. Moore, Scale: Landscape attributes and geographical information systems, *Hydrol. Processes, 9*, 401-422, 1995.

Bartholomew, J.C., P.J.M. Geelan, H.A.G. Lewis, P. Middleton, and B. Winkleman (Eds.), *The Times Atlas of the World: Comprehensive Edition*, Times Books, London, 1994, 1988.

Baumgartner, A., and E. Reichel, *The World Water Balance: Mean Annual Global, Continental and Maritime Precipitation, Evaporation and Runoff*, Elsevier Sci., New York, 1975.

Beven, K., and E.F. Wood, Flow routing and the hydrological response of channel networks, in *Channel Network Hydrology*, edited by K. Beven and M.J. Kirkby, pp. 99-128, John Wiley, New York, 1993.

Billen, G., J. Garnier, and P. Hanset, Modelling phytoplankton development in whole drainage networks: The RIVERSTRAHLER model applied to the Seine River system, *Hydrobiologia, 289*, 119-137, 1994.

Burrough, P.A., *Principles of Geographical Information Systems for Land Resources Assessment, Monographs on Soils and Resources Survey 12*, 193 pp., Oxford Univ. Press, New York, 1986.

Coe, M.T., Simulating continental surface waters: An application to Holocene northern Africa, *J. Clim., 10*, 1680-1689, 1997.

Coe, M.T., A linked global model of terrestrial hydrologic processes: Simulation of rivers, lakes, and wetlands, *J. Geophys. Res., 103*(D8), 8885-8899, 1998.

Covich, A.P., Water and ecosystems, in *Water in Crisis: A Guide to the World's Fresh Water Resources*, edited by P.H. Gleick, pp. 40-55, Oxford Univ. Press, New York, 1993.

Defense Mapping Agency Aerospace Center (DMAAC), Operational Navigation Charts, 1:1 M scale, St. Louis, Mo., 1980-1986.

Dingman, S.L., Drainage density and streamflow: A closer look, *Water Resour. Res., 14*, 1183-1187, 1978.

Dingman, S.L., *Physical Hydrology*, Prentice-Hall, Englewood Cliffs, N.J., 1994.

Dubief, J., *Essai sur l'Hydrologie Superficielle au Sahara*, PhD Thesis, Faculté des Sciences, Université d'Alger, 1953.

Dynesius, M., and C. Nilsson, Fragmentation and flow regulation of river systems in the northern third of the world, Science, *266*, 753-762, 1994

Edwards, M., Global gridded elevation and bathymetry (ETOPO5), Digital raster data on a 5-minute geographic grid, NOAA Nat. Geophys. Data Cent., Boulder, Colo., 1989.

Environment Canada, Hydat Version 4.93, Surface Water and Sediment Data, Atmos. Environ. Serv., Ottawa, Canada, 1994.

Environmental Systems Research Institute (ESRI), *ARC/World 1:3 M Digital Data on CD-ROM: Users Guide and Data Reference*, Edition 1, Redlands, Calif., 1992.

Environmental Systems Research Institute (ESRI), *Digital Chart of the World for Use with ARC/INFO Software, Data Dictionary, 1:1 M ARC/INFO Digital Data on CD-ROM*, Redlands, Calif., 1993.

Esser, G., and G.H. Kolhmaier, Modelling terrestrial sources of nitrogen, phosphorus, sulphur, and organic carbon in rivers, in *Biogeochemistry of Major World Rivers*, SCOPE 42, edited by E. Degens, S. Kempe, and J.E. Richey, pp. 297-322, John Wiley, New York, 1991.

Fekete, B.M., C.J. Vörösmarty, and W. Grabs, *Global, Composite Runoff Fields Based on Observed River Discharge and Simulated Water Balances, Rep. 22*, Global Runoff Data Center (GRDC), Koblenz, Germany, 1999.

Grabs, W., T. DeCouet, and J. Pauler, *Freshwater Fluxes from Continents into the World Oceans Based on Data of the Global Runoff Data Center, Rep. 10*, Global Runoff Data Center (GRDC), Koblenz, Germany, 1996.

Graham, S.T., F.S. Famiglietti, and D.R. Maidment, Five-minute, ½°, and 1° data sets of continental watersheds and river networks for use in regional and global hydrologic and climate system modeling studies, *Water Resour. Res., 35*, 583-587, 1999.

Hagemann, S., and L. Dümenil, A parameterization of the lateral waterflow for the global scale, *Clim. Dyn., 14*, 17-31, 1998.

Hartmann, D.L., *Global Physical Climatology*, 408 pp., Academic, San Diego, Calif., 1994.

Horton, R.E., Erosional development of streams and their drainage basins: Hydrophysical approach to quantitative morphology, *Geol. Soc. Am. Bull., 56*, 281-300, 1945.

Jenson, S., Application of hydrologic information automatically extracted from digital elevation models, *Hydrol. Processes, 5*, 31-44, 1991.

Kaczmarek, Z., et al., Water resources management, in *Climate Change 1995: Impacts, Adaptations, and Mitigation of Climate Change*, edited by R.T. Watson et al., Chap. 14, Cambridge Univ. Press, New York, 1996.

Kirkby, J.J., Tests of a random network model and its application to basin hydrology, *Earth Surf. Processes, 1*, 197-212, 1976.

Kite, G.W., A. Dalton, and K. Dion, Simulation of streamflow in a macroscale watershed using general circulation model data, *Water Resour. Res., 30*, 1547-1559, 1994.

Korzoun, V.I., A.A. Sokolov, M.I. Budyko, K.P. Voskresensky, G.P. Kalinin, A.A. Konoplyantsev, E.S. Korotkevich, and M.I. L'vovich, (Eds.), *Atlas of World Water Balance and Water Resources of the Earth*, USSR Committee for the International Hydrological Decade, Leningrad, 1978

Leopold, L.B., M.G. Wolman, and J.P. Miller, *Fluvial Processes in Geomorphology*, 522 pp., W.H. Freeman, New York, 1964.

Liston, G.E., Y.C. Sud, and E.F. Wood, Evaluation of GCM land surface hydrology parameterizations by computing river discharges using a runoff model: Application to the Mississippi Basin, *J. Appl. Meteorol., 33*, 394-405, 1994.

Ludwig, W., and J.-L. Probst, River sediment discharge to the oceans: Present-day controls and global budgets, *Am. J. Sci., 298*, 265-295, 1998.

Ludwig, W., J.L. Probst, and S. Kempe, Predicting the oceanic input of organic carbon by continental erosion, *Global Biogeochem. Cycles, 10*, 23-41, 1996a.

Ludwig, W., P. Amiotte-Suchet, and J.L. Probst, River discharges of carbon into the world's oceans: Determining local inputs of alkalinity and of dissolved and particulate organic carbon, *C. R. Acad. Sci., 323*, 1007-1014, 1996b.

L'vovich, M.I., and G.I. White, Use and transformation of terrestrial water systems, in *The Earth as Transformed by Human Action*, edited by B.L. Turner et al., pp. 235-252, Cambridge Univ. Press, New York, 1990.

Meybeck, M., Global distribution of lakes, in *Physics and Chemistry of Lakes*, 2nd ed., edited by A. Lerman, D. Imboden, and J. Gat, pp. 1-35, Springer-Verlag, New York, 1995.

Meybeck, M., and A. Ragu, *GEMS/Water Contribution to the Global Register of River Inputs (GLORI)*, Provisional Final Report, 245 pp., United Nations Environment Programme/WHO/UNESCO, Geneva, Switzerland, 1995.

Meybeck, M., and A. Ragu, Presenting the GEMS-GLORI, a compendium for world river discharge to the oceans, *IAHS Publ., 243*, pp. 3-14, 1997.

Miller, J., and G.L. Russell, The impact of global warming on river runoff, *J. Geophys. Res., 97*, 2757-2764, 1992.

Milliman, J.D., and J.P.M. Syvitski, Geomorphic/tectonic control of sediment discharge to the ocean: The importance of small mountainous rivers, *J. Geol., 100*, 525-554, 1992.

Mintz, Y., and Y.V. Serafini, *Global Monthly Climatology of Soil Moisture and Water Balance*, Lab. de Meterol. Dyn., Ecole Polytechnique, Paris, 1989.

Naden, P.S., A routing model for continental-scale hydrology, in *Macroscale Modelling of the Hydrosphere, IAHS Publ. 214*, 67-79, 1993.

Oki, T., K. Musiake, H. Matsuyama, and K. Masuda, Global atmospheric water balance and runoff from large river basins, *Hydrol. Processes, 9*, 655-678, 1995.

Oki, T., and Y. C. Sud, Design of Total Runoff Integrating Pathways (TRIP) - A global river channel network, *Earth Inter., 2*, 1998. (Available at http://EarthInteractions.org)

Postel, S.L, G.C. Daily, and P.R. Ehrlich, Human appropriation of renewable fresh water, *Science, 271*, 785-788, 1996.

Roads, J.O., S.-C. Chen, A. Guetter, and K. Georgakakos, Large-scale aspects of the United States hydrologic cycle, *Bull. Am. Meteorol. Soc., 75*, 1589-1610, 1994.

Sausen, R., and L. Dümenil, A model of river runoff for use in coupled atmosphere-ocean models, *J. Hydrol., 155*, 337-352, 1994.

Seitzinger, S. P., and C. Kroeze, Global distribution of nitrous oxide production and N inputs in freshwater and coastal marine ecosystems, *Global Biogeochem. Cycles, 12*, 93-113, 1998.

Shiklomanov, I.A., *Assessment of Water Resources and Water Availability in the World*, 127 pp., State Hydrol. Inst., St. Petersburg, Russia, 1997.

State Hydrological Institute, Russian National Water Resources Data Bank, Data supplied by I. Shiklomanov, Director, SHI, St. Petersburg, Russia, 1997.

Strahler, A.N., Quantitative analysis of watershed geomorphology, *Trans. Am. Geophys. Union, 38*, 913-920, 1957.

Strahler, A.N, Quantitative geomorphology of drainage basins and channel networks, in *Handbook of Applied Hydrology*, section 4-II, edited by V.T. Chow, McGraw-Hill, New York, 1964.

United Nations Educational, Scientific, and Cultural Organization-International Hydrological Programme (UNESCO-IHP), *Discharge of Selected Rivers of the World*, UNESCO-IHP, Paris, 1965-1984.

United Nations Educational, Scientific, and Cultural Organization-International Hydrological Programme (UNESCO-IHP), *Discharge of Selected Rivers of Africa*, UNESCO-IHP, Paris, 1995.

U.S. Geol. Surv. (USGS), *U.S. GeoData Digital Elevation Models: Data User Guide 5*, National Mapping Program, 51 pp., Reston, Virginia, 1990.

U.S. Geol. Surv. (USGS), *Water Resources Data for Alaska, Water Years 1966-1995: Water-Data Rep. AK 66-1 to AK 95-1* (published annually), U.S. Dept. of the Interior, Geological Survey, National Technical Information Service, Springfield, Virginia, 1967-1996.

Vörösmarty, C. J., B. Moore, A.L. Grace, M.P. Gildea, J. M. Melillo, B.J. Peterson, E.B. Rastetter, and P. A. Steudler, Continental scale models of water balance and fluvial transport: An application to South America, *Global Biogeochem. Cycles, 3*, 241-265, 1989.

Vörösmarty, C. J., B. Moore, A. Grace, B. J. Peterson, E. B. Rastetter and J. Melillo, Distributed parameter models to analyze the impact of human disturbance of the surface hydrology of a large tropical drainage basin in southern Africa, in *Hydrology for the Water Management of Large River Basins, IAHS Publ. 201*, 233-244, 1991.

Vörösmarty, C.J., C.J. Willmott, B.J. Choudhury, A.L. Schloss, T.K. Stearns, S.M. Robeson, and T.J. Dorman. Analyzing the discharge regime of a large tropical river through remote sensing, ground-based climatic data, and modeling, *Water Resour. Res., 32*, 3137-3150, 1996a.

Vörösmarty, C.J., B. Fekete and B.A. Tucker, *Global River Discharge Data Base*, Version 1.0 (RivDIS v1.0), vol. 0 through 6, A contribution to IHP-V Theme 1, Technical Documents in Hydrology Series, United Nations Educational, Scientific, and Cultural Organization, Paris, 1996b.

Vörösmarty, C.J., R. Wasson, and J.E. Richey (Eds.), *Modeling the Transport and Transformation of Terrestrial Materials to Freshwater and Coastal Ecosystems, IGBP Rep. 39*, International Geosphere-Biosphere Program Secretariat, Stockholm, 1997a.

Vörösmarty, C.J., K. Sharma, B. Fekete, A.H. Copeland, J. Holden, J. Marble, and J.A. Lough, The storage and aging of continental runoff in large reservoir systems of the world, *Ambio, 26*, 210-219, 1997b.

Vörösmarty, C.J., M. Meybeck, B. Fekete, and K. Sharma, The potential impact of neo-Castorization on sediment transport by the global network of rivers, in *Human Impact on Erosion and Sedimentation*, edited by D. Walling and J.-L. Probst, *IAHS Publ. 245*, Wallingford, U.K., 1997c.

Vörösmarty, C.J., B. Fekete, and B.A. Tucker, Global River Discharge Database, Version 1.1 (RivDIS v1.0 supplement), [Available on-line through the Institute for the Study of Earth, Oceans, and Space/University of New Hampshire, Durham NH, USA, at http://www.watsys.unh.edu], 1998a.

Vörösmarty, C.J., C.A. Federer, and A. Schloss, Potential evaporation

functions compared on U.S. watersheds: Implications for global-scale water balance and terrestrial ecosystem modeling, *J. Hydrol., 207*, 147-169, 1998b.

White, D.A., R.A. Smith, C.V. Price, R.B. Alexander, and K.W. Robinson, A spatial model to aggregate point-source and non-point source water quality data for large areas, *Comput. Geosci., 18*, 1055-1073, 1992.

Willmott, C. J., C. M. Rowe, and Y. Mintz, Climatology of the terrestrial seasonal water cycle, *J. Clim., 5*, 589-606, 1985.

B.M. Fekete, R.B. Lammers, and C.J. Vörösmarty, Institute for the Study of Earth, Oceans, and Space, University of New Hampshire, Durham, NH 03824. (charles.vorosmarty@unh.edu)

M. Meybeck, UMR SISYPHE CNRS, Université de Paris VI, Place Jussieu, 75257 Paris, France.

(Received November 11, 1998; revised April 13, 1999; accepted April 28, 1999.)